UNIVERSITÈ KASDI MARBEH OUARGLA
FACULTY OF HYDROCARBONS RENEWABLE ENERGIES AND EARTH AND UNIVERSE SCIENCES
DEPARTMENT OF EARTH AND UNIVERSE SCIENCES

MEMORY

Submitted for the MASTER diploma

Speciality: Geology.

Option: Hydrocarbon geology

THÈME

Implication of lithofacies types and petrophysical characteristics on the quality of the Triassic reservoir in the southern Benkahela zone

Presented by:

- Kious Mohammed ride

- Bekkouche Mohammed Mohcen

- Driche ayoub

Name and title	Rank	University	Adjective
Mr. HACINIMessaoud	Professor of Higher Education	University of Ouargla	President
Mr. MEBROUKI Nassira			Admin
Mr sahri leila			Discussor

Academic year: 2024/2025

Dedications

We, Redha Mohcen Ayoub

We dedicate this work to those who have played a major role in our success,

to those who have provided us with unwavering support, love, and guidance, and who have been our true pillars throughout our academic journey.

To our dear parents,

*Y*ou instilled in us the values of hard work and diligence, and taught us that knowledge is the path to success.

We will never forget your sacrifices and efforts; you are the reason we have reached this moment. This success is also your success.

To our dear brothers and sisters,

Thank you for every moment of support and for your unwavering encouragement.

You have always been our source of strength during difficult times.

To our loyal friends,

I would especially like to thank Yassin, Ayman, Fares, Nouri, Mustika, Tayeb, Hayat, and everyone who has stood by us throughout this journey and contributed to making our path easier and brighter.

You are the ones who made our academic journey enjoyable, and we will never forget your support.

To our esteemed teachers,

who have guided us along this path and who have put in great effort in educating us and preparing us for our future, we extend our deepest gratitude and appreciation.

To everyone who has helped and supported us,

we express our sincere appreciation and gratitude. Without you, we would not have reached this point

شكر وتقدير

قال عز وجل: " يرفع الله الذين آمنوا منكم والذين أوتوا العلم درجات والله بما تعملون خبير "

اللهم لك الحمد على ما أعنتنا عليه وأنعمت علينا به وعلى ماهديتنا اليه على الأصل نمشي والأصل يدفعنا أن نرد الفضل لأصحابه، وأن نسدي الشكر لمستحقيه ممن أفادونا ولو بكلمة طيبة.

أولا نتقدم بخالص الشكر للأستاذة المشرفة " مبروكي نصيرة " على متابعته لهذا البحث وعلى توجيهاتها القيمة ونصائحها الهادفة..

ونتقدم بشكرنا الخاص إلى جميع أساتذة جيولوجيا وتوجيهاتهم لنا لهم كل التقدير والاحترام.

ولا يفوتنا ان نقدم العرفان التام إلى كل من ساعدنا من قريب او بعيد في إنجاز هذا العمل.

نسأل الله سبحانه وتعالي أن يجعل ذلك في ميزان حسناتهم جميعنا.

Liste des Abréviations

Abréviation	Signification
API	American Petroleum Institute (densité du pétrole)
CFPA	Compagnie Française des Pétroles Algérie
DLCC	Département Carothèque Centrale
DRT	Discrete Rock Type (Type de roche discrète)
FZI	Flow Zone Indicator (Indicateur de zone d'écoulement, en µm)
GOR	Gas-Oil Ratio (Rapport gaz-pétrole)
NPI	Normalized Porosity Index (Indice de porosité normalisé)
RQI	Reservoir Quality Index (Indice de qualité du réservoir, en µm)
R35	Effective Pore Radius (Rayon effectif des pores, en µm)
S1, S3, S4	Niveaux salifères du Trias et du Lias
TAG	Trias Argilo-Gréseux (Clay-Sandstone Triassic)
TAGS	Trias Argilo-Gréseux Supérieur (Upper Clay-Sandstone Triassic)

List of Tables

List of Figures

Table of Contents

INTRODUCTION GENERAL

INTRODUCTION GENERAL

The Saharan platform to which our study region belongs is located to the south of alpine Algeria and belongs to the North African Craton. It comprises a Precambrian basement on which lies a powerful unconformity of sedimentary cover, structured in the Palaeozoic into several basins separated by high zones:

- The Tindouf and Reggane basins on the northern and north-eastern edges of the Reguibat shield. The sedimentary cover reaches 8,000 m in the Tindouf basin and 6,500 m in the Reggane basin. In this little-explored area, the Palaeozoic formations could contain liquid and gaseous hydrocarbons;

- The Béchar basin, bounded to the north by the High Atlas and to the south and west by the Ougarta chain. Its sedimentary cover is thought to reach 8,000m. The reservoirs are found in the lower Paleozoic detritic and Carboniferous reefs;

- The Ahnet-Timimoun basin, which is bounded to the north by the Oued Na mous shoal, to the west by the Ougarta chain, to the south by the Tuareg shield and to the east by the Idjerane-M'zab ridge. Coverage averages 4,000m. In the south, the Ordovician and Lower Devonian reservoirs are gas-bearing. In the north, in the Sbâa basin, oil has been discovered throughout the Palaeozoic;

- The Mouydir and Aguemour-Oued M'ya basins are bounded to the west by the Idjerane-M'zab ridge and to the east by the Amguid-El Biod ridge. In the south, Palaeozoic sediments outcrop in the Mouydir. To the north, in the Aguemour-Oued M'ya depression, filled in by a powerful Palaeozoic and Meso-Cenozoic series (5000m at Oued M'ya). Major deposits have been discovered in the Cambrian (Hassi Messaoud) and Triassic (HassiR'Mel);

- The Illizi-Ghadamès synclise is bounded to the west by the Amguid-El Biod ridge and to the east by the Tihemboka mole and the Tunisian-Libyan border. In the Ghadamès basin, the sedimentary cover (over 6,000 m) contains hydrocarbon deposits in the Paleozoic and Triassic (SONATRACH/ EXPLOTATION, 1995).

Chapter I : Regional and Local Context of the Oued M'ya Basin and the Benkahla reservoir

1. Regional context of the Oued M'ya basin

I.1.1. Geographical location of the Oued M'ya

The Oued M'ya is a basin on the Saharan platform, corresponding to the western part of the Triassic province, covering an area of 400,000 km2, The geographical limits are presented as the best landmarks (Figure 01).

Parallels 31˚15' and 33˚00' respectively limit together south and north, and meridians 6˚15' and 3˚30' limit east and west, encompassing blocks :438-425- 422-437-436-3178-420-419-418-417and416, belonging to Sonatrach district IV. The basin is bounded by the Djemaa-Touggourt high structure to the north, the Mouydir basin to the south, the Amguid-Messaoud high structure to the east and the Allal vault to the west (Figure 01).

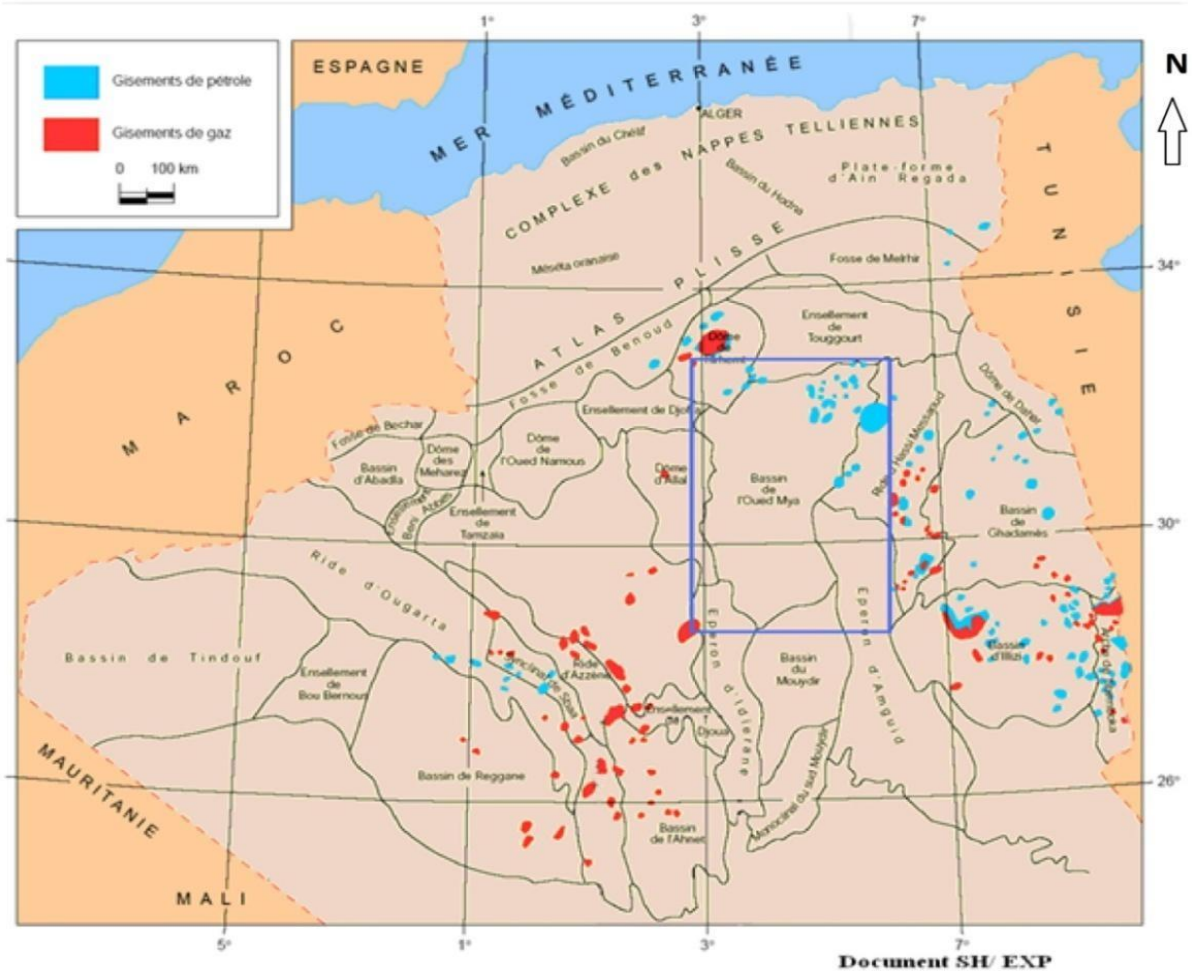

Figure 01: Geographical location of Oued Mya (SONATRACH/ EXPLOTATION, 1995)

.1.2.Geological setting of the Oued Mya basin

The Oued M'ya region is merely an intracratonic sub-basin. Its northern edge progressively slopes towards the Saharan flexure where the existence of a very subsident trough in the Mesozoic gave rise to the pericratonic chain of the Saharan Atlas (Figure 02).

The evolution of the Oued Mya region since the Cambrian comprises two major stages:

1- Paleozoic sedimentation, practically restricted to the Lower Paleozoic and its pre-Hercynian structuring;

2- The creation of a basin in the Triassic and its evolution during the Mesozoic and Tertiary periods.

These two main stages in the region's history lead us to consider two sedimentary megacycles, the Palaeozoic and the Mesozoic, classically separated by the Hercynian unconformity, with the high zones structuring

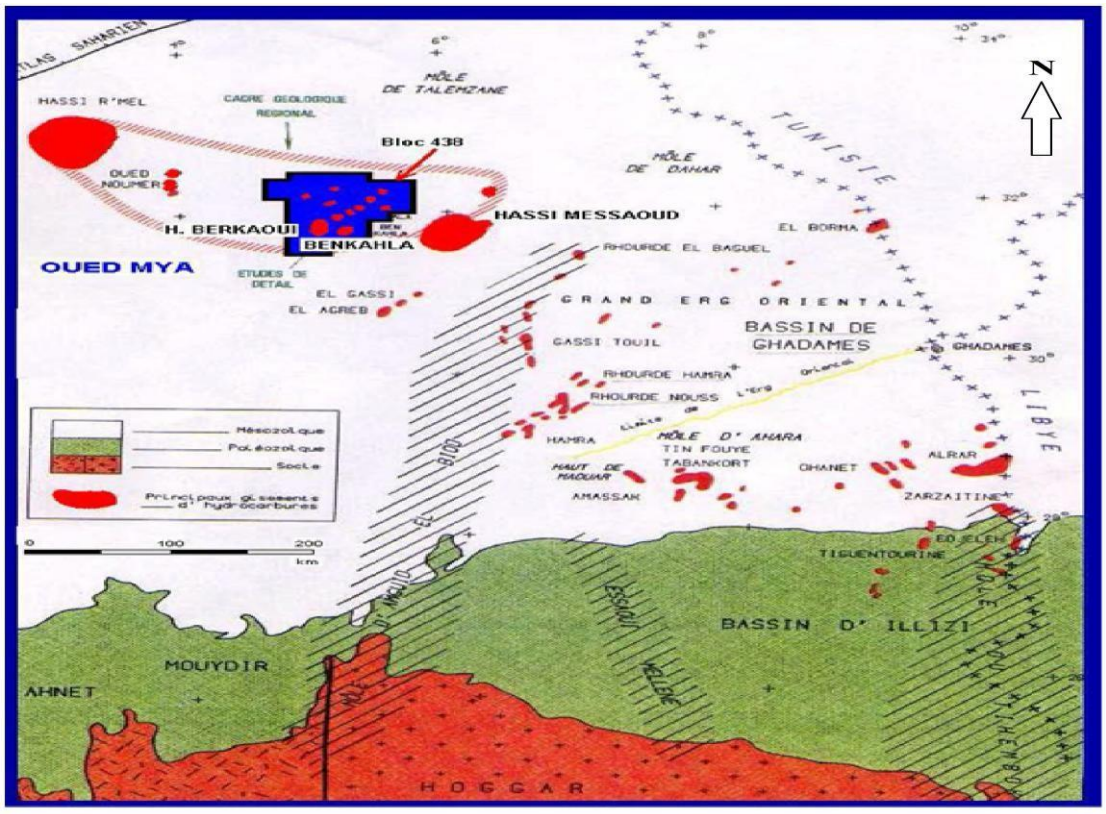

Figure 02: Geological situation of the Oued Mya basin (SONATRAH/ PRODUCTION)

1.2.1. Stratigraphy

In the northern part of the platform (Oued M'ya), the typical sedimentary series, up to 6,000 metres thick (Figure 03), consists of Palaeozoic deposits, often eroded down to Ordovician and Cambrian age.

The Mesozoic, which is discordant with the Palaeozoic, is present from the Triassic to the Cretaceous.

The Cenozoic is represented by a thin detrital series from the Miocene to the Pliocene (SONATRACH and SCHLUMBERGER, 2007).

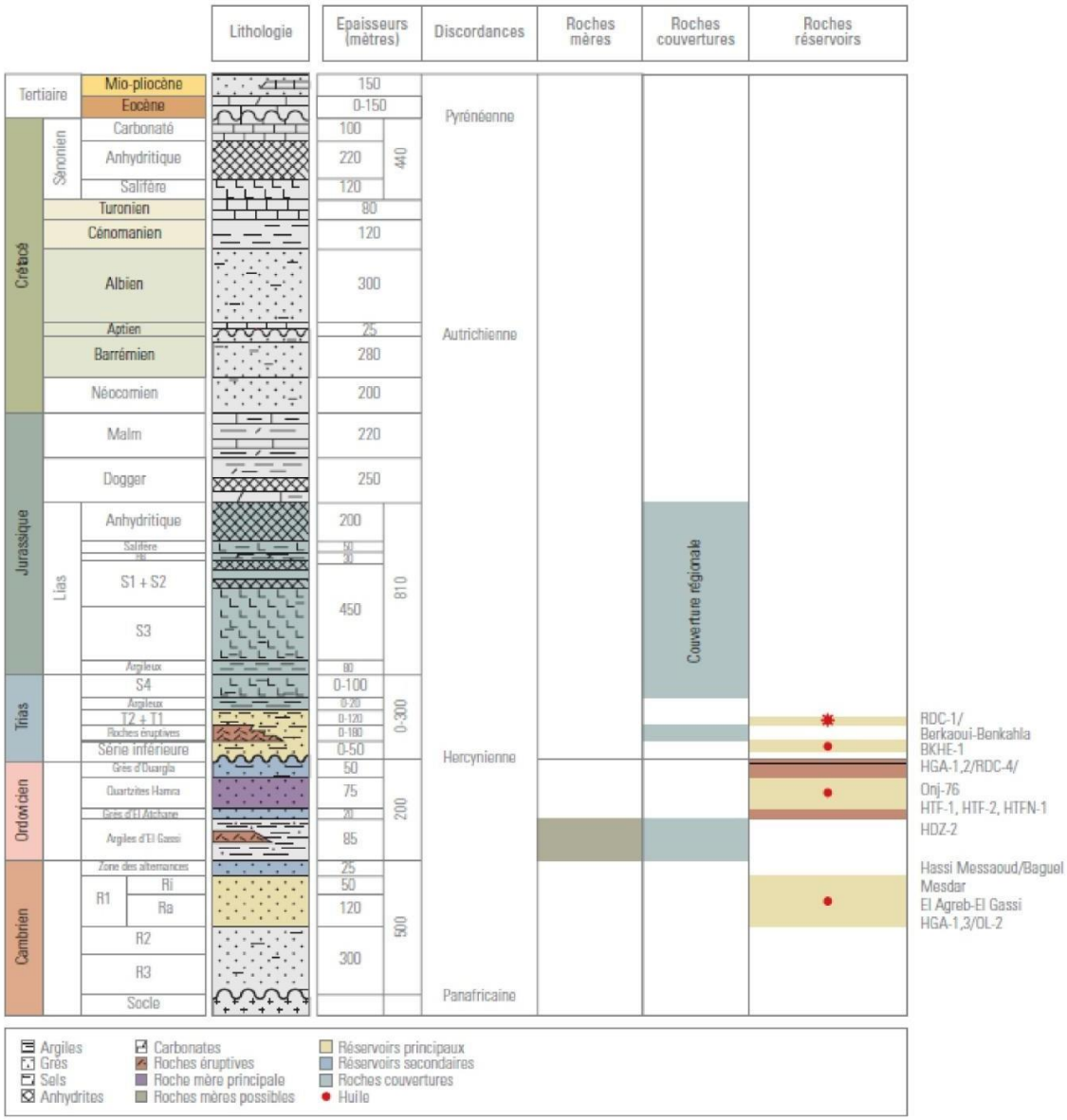

Figure 03: Typical lithostratigraphic section of the Wadi Mya basins (SONATRACH and SCHLUMBERGER, 2007).

I.1.2.2. Tectonics

I.1.2.2.A. The main stages in the structural evolution of the Saharan platform in the Palaeozoic

In view of the reduction in thickness and even the complete disappearance of sedimentary units as a result of local unconformities or lack of sedimentation, it is necessary to recall the main phases in the structural evolution of the Saharan platform during the Palaeozoic (Table 01).

I.1.2.2.A.1.The Pan-African orogeny and the origin of the fracturing network of the North African craton

Materialised by vertical movements accompanied by volcanic eruptions and uplift, leading to the erosion of the sedimentary cover. The result of this orogeny is the fracturing network.

I.1.2.2.A.2.Distension of the Cambro-Ordovician and establishment of the cover,

resulting in the formation of a pediplain, known as the Infra-Tassilian.

I.1.2.2.A.3.The Taconic compression phase (Caradoc)

After the period of distension followed by the generalised transgression of the Arenigian - Lianvirian, the Caradoc saw a compressive movement, accompanied by regional uplift leading to erosion. At the same time, climate change led to the formation of an ice cap centred on the central Sahara of Caradoc-Asligillian age.

I.1.2.2.A.4.Melting of the ice sheet and eustatic rejeux

The melting of the ice sheet during the Upper Ordovician led to a rise in sea level.

I.1.2.2.A.5.The Caledonian compression phase

This took place at the end of the Silurian and was oriented east-west.

I.1.2.2.A.6- The Lower Devonian distension phase

After the distension movements, there was a marine transgression in the Emsian.

I.1.2.2.A.7. Upper Middle Devonian tectonic movements

Materialised by the north-south trending Frasnian unconformity.

I.1.2.2.A.8. Post-Famennian movement

I.1.2.2.A.9. Hercynian movements

According to the study (A. BOUDJEMAA 1987), two Hercynian movements have been identified:

- Early Hercynian movements

In the Tournaisian -Visean with a N40° direction of tightening.

- Major Hercynian movements

Having caused the complete cessation of Carboniferous sedimentation. The axis of the folds and the measurements of the striations give a clamping direction of N120°.

Table 01: Tectonic phases affecting the Saharan platform. (A. Boujemaa, 1987).

PERIODE MAX D'ACTIVITE	DIRECTION DE LA CONTRAINTE	EFFET SUR LE SYSTEME DE FAILLES	EFFET SUR LA SEDIMENTATION
PANAFRICAINE	E-W 	Brittle tectonics creating conjugate NW-SE & NE-SW faults and fractures	Compartmentalization of the Central Sahara Craton
CAMBRO-ORDOVICIENNE E	NW-SE 	Normal movement along N-S faults	Thickness variations controlled by faults; NW tilting of the Saharan platform; Volcanism
TACONIQUE (Caradoc-Ashgilien)	E-W 	Reverse movement along resulting N-S faults	Formation of N-S structures; uplift of the Reguibat and Tuareg shields
CALEDONIENNE (Siluro-Dévonien)	E-W 	Reverse or strike-slip movement along N-S faults	Erosion along high zones with N-S & E-W orientation (Tihemboka, Ahara)
FRASNIEN	NW-SE 	Normal movement along NE-SW faults	Non-deposition and local erosion (Ahara high); Volcanism
VISEEN (Hercynienne précoce)	N40° 	Reverse or strike-slip movement along N-S faults; start of Variscan chain formation	Erosion of Tihemboka; uplift of Ougarta
CARBONIFERE SUP. À PERMIEN (Hercynienne principale)	N120° 	Reverse or strike-slip movement along NE-SW faults (related to Pangaea formation)	Erosion along NE-SW axes
RIFTING TRIAS-LIAS (Dislocation de la Pangée)	NW-SE 	Reactivation of NE-SW faults ending at TAGS and S4	Sedimentation controlled by faults, causing rapid thickness variations along NE-SW faults
CRETACE INFERIEUR (Autrichienne)	E-W 	Reactivation of strike-slip faults N-S & NE-SW due to differential movement between European and African plates	Erosion of Cretaceous sediments below the Aptian (Al Biod & Illizi arches); minor impact on Berkine Basin
EOCENE (Pyrénéenne)	N-S & NW-SE 	Beginning of thrusting in the north due to African-European plate convergence; strike-slip on South Atlas fault	—
MIOCENE	NW-SE & N-S 	Major compression event in the Atlas domain	Predominantly flysch sedimentation in the north
POST-VILLAFRANCHIEN	N-S 	Tilting and block inversion; final compression phase in the Atlas domain	Major collision event; uplift of the Hoggar; tilting of El Borma block

The present architecture is the result of a long evolution, the culmination of slow deformations which have continued more or less continuously throughout the history of the basin.

The main phases of deformation that have influenced the sedimentation and lastructuration of the basin (Boeuf, 1971; Boudjemaa, 1987) are the Hercynian phase and the Austrian phase.

The Hercynian movements correspond to compression in the direction

N° 120, with the most significant deformation occurring along the NE-SW faults.

One of the most important features of this formation concerns the fate of the main parent rocks (Silurian). They are preserved in the Berkine and Oued M'ya depressions, and will supply hydrocarbons to the structural and stratigraphic traps which will form later. (Boudjemaa, 1987).

During the Austrian movements (terminal Aptian), there was an east-west phase of compression, which caused the N-S submeridian faults of the Oued M'ya to be replayed in reverse.

This compression is thought to be responsible for the individualisation of the structural traps.

I.1.2.2.B. Structural evolution of the Oued Mya basin

The main structural elements run in a N-S and NE-SW direction (figure 04). (SH and Sch, 2007).

Cambrian: Significant erosion levelled the previous structures and relief (Boeuf et al, 1971).

The Oued M'ya centre area was located on the flank of a major depression which corresponded to the current location of the Hassi Messaoud high zone (Benamrane, 1993).

The Ordovician period began with a marine transgression of the Arénigien-Lianvirinien, with regional uplift (Eglab). These uplifts led to erosion, sometimes reaching the bedrock (Boeuf, 1971). Towards the end of this period, an ice age set in, with a cap at the level of the present-day Hoggar.

Following the Caledonian phase, the central Oued M'ya area began to rise while remaining submerged.

In the Silurian, the definitive melting of this ice cap led to a rise in sea level, and a generalised transgression reached the southern Sahara where black graptholite clays were deposited (Boudjemaa, 1987)

At this time, the Oued M'ya centre area was entirely covered by this sea (Benamrane et al, 1993).

In the Devonian, following tectonic uplift (Caledonian phase), a regression of the sea during the Geddinian was followed by a transgression.

The onset of the Hercynian orogeny, and the gradual uplift of the HassiMessaoud area, led to the displacement of deposits from the centre of the basin towards the west, where Devonian deposits developed.

Towards the end of the Carboniferous, the collision between Gondwana and Laurasia accentuated the uplift of the Tilghermt dome region and the structuring of Djemaa Touggourt.

The Oued M'ya region appeared to be a submerged high plateau, which prevented the deposition of the Carboniferous (Benamrane, et al, 1991). The formation of Pangea took place towards the end of the Hercynian orogeny and the intense erosion of the relief reached the basement in places.

At Oued M'ya, the Devonian is the youngest Paleozoic formation. In the Permo-Triassic, the region remained continental until the end of the Triassic, which meant that the Permian Sea did not reach the area.

During the Triassic, the Oued M'ya area was characterised by a fluvial system set up against the Hercynian palaeovalleys, running in a NE-SW direction, with sources of supply constituted by the high areas of the time, which were Hassi R'mel, Hassi Messaoud and the Allal vault.

At the end of the Triassic, evaporitic deposits were followed by carbonates on this submerged land, then by a marine transgression in the Upper Jurassic.

In the Cretaceous, a manifestation of the Alpine orogeny and a marine transgression took place over a large area, followed by a regression in the Albian.

Following the widespread transgressions of the Cenomanian and Turonian, Alpine orogenic movements shaped the current structure.

The Oued M'ya area is currently characterised by a fairly complex structure inherited from the Paleozoic era, with NE-SW trending structural features (Figure 05).

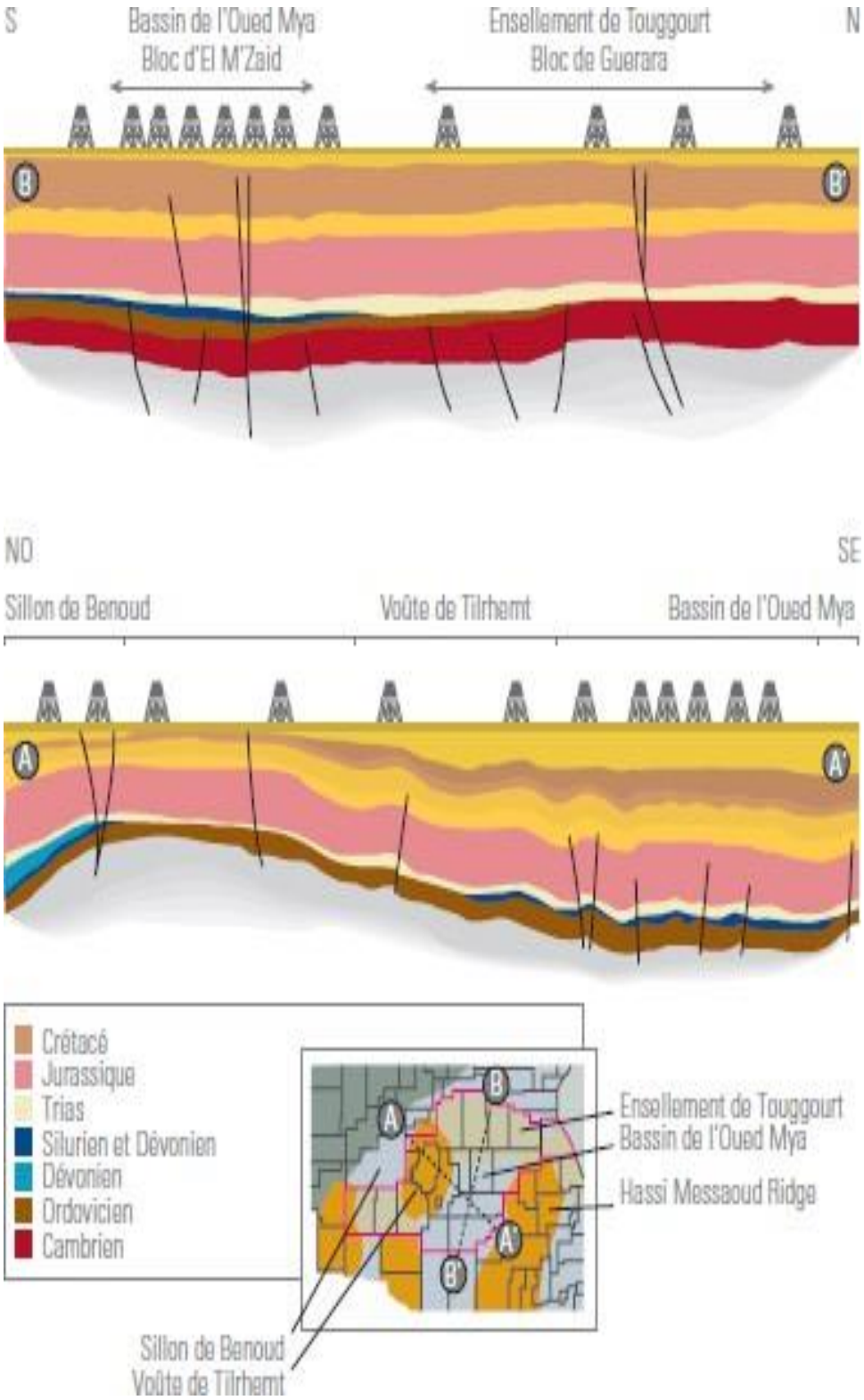

Figure 04: N-S and NW-SE geological section of the Wadi Mya basin (SONATRACH and SCHLUMBERGER, 2007).

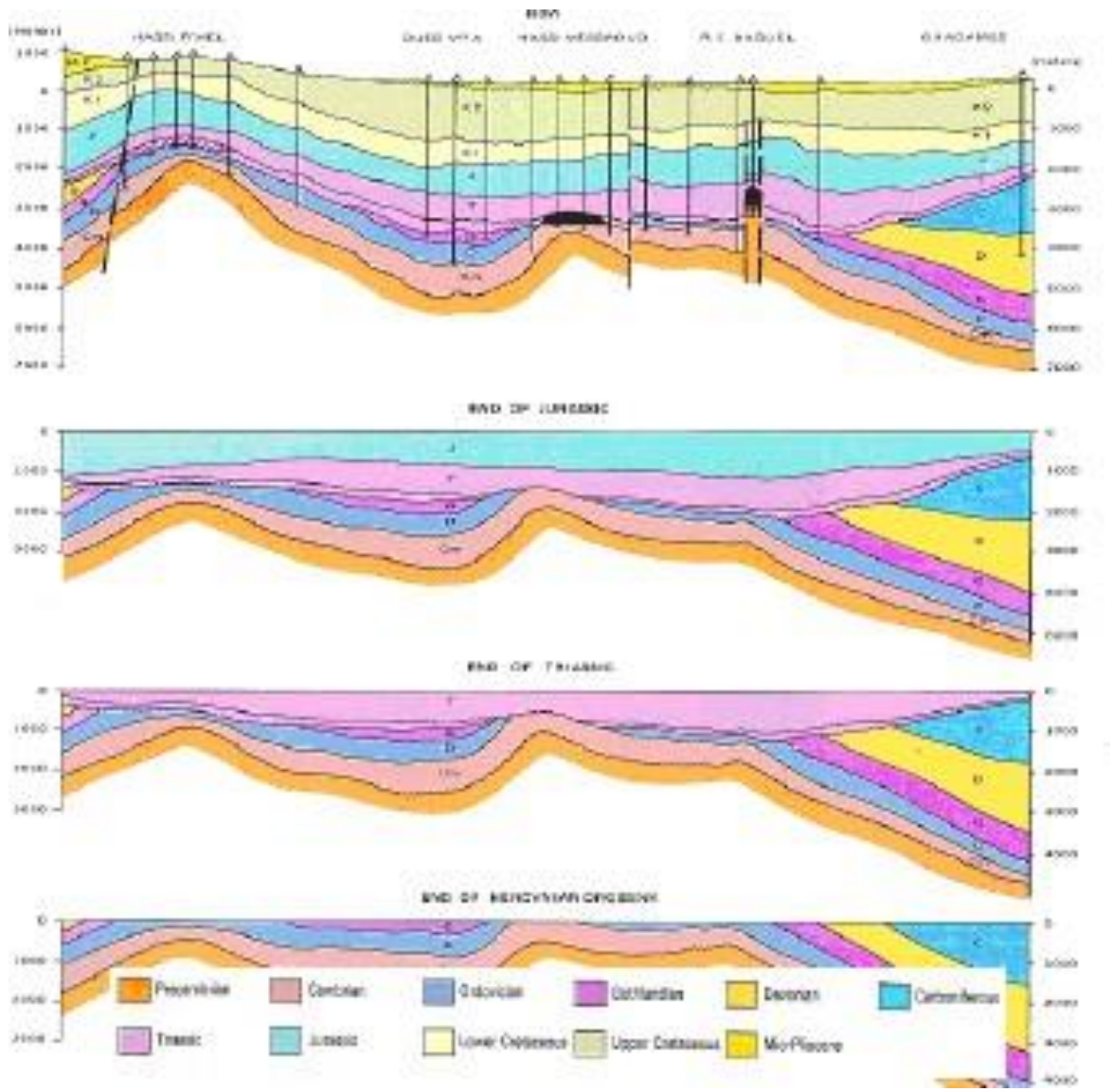

Figure 05: The different tectonic phases over geological time (after Boujemaà, 1987).

I.1.2.3. Petroleum potential of the Oued Mya basin

The major petroleum potential of the basin lies in the presence of Triassic reservoirs. However, the Paleozoic evolution of the basin is the key to understanding the petroleum results obtained to date and providing guidance for exploitation.

The Oued M'ya depression is in fact characterized by the presence of a residual Paleozoic series, containing the well-developed, organic-rich Silurian-age radioactive clays that constitute the main bedrock, unfortunately eroded over large areas of the region. This series is overlain by a powerful Mesozoic series comprising at its base the main reservoirs of the basin and their saliferous cover (Trias-lias).

I.1.2.3.A. Source rocks

The Silurian is the main source rock level in the Oued M'ya basins, thanks to a basal level of black-gray to black radioactive clays, very rich in organic matter (SONATRACH and SCHLUMBERGER, 2007).

I.1.2.3.B. Wadi M'ya reservoirs (SONATRACH and SCHLUMBERGER, 2007)

I.1.2.3. B.1.Main reservoirs

In the basin, the Triassic fluviatile sandstones include:

- The lower series unit (center of the basin and south of HassiR'mel) ;

- Unit T1 (north of the central part of the basin and HassiR'mel region);

- Unit T2 (HassiR'mel region).

Quartzite sandstones of the Hamara quartzite unit (orodovician) considered as the main target since the recent discovery of oil in the Berkaoui structure (BKP well).

. The secondary reservoirs are

- Lower Devonian sandstones, Ordovician quartzite sandstones (M'kratta slab, Oued Saret sandstone, Ouargla sandstone, El Atchane sandstone) and Cambrian sandstones;

- Muscovite sandstones and carbonates to the NW of the basin and Jurassic carbonates to the NE.

I.1.2.3.C. Regional coverage of Triassic reservoirs

This is made up of Triassic (S4 saliferous) and Lias (S3 to S1 levels) evaporites. Paleozoic reservoirs are covered by intercalated clay series.

I.1.2.3.D. Trapping in the basin

Trapping is structural, mixed or purely stratigraphic. Thereservoirs are fed vertically by faults and/or laterally along the drains formed by the reservoir levels (SONATRACH and SCHLUMBERGER, 2007).

I.1.3. Petroleum system (SONATRACH and SCHLUMBERGER, 2007) Triassic reservoir

In the Oued M'ya basin, the Triassic clay-sandstone corresponds to an azoic detritic unit, overlain by evaporitic deposits of the Saliferous Triassic S4, resting in angular unconformity on formations of variable age from Cambrian to Lower Devonian. The Triassic is bounded at the base by the Hercynian discordance and at the

Summit by the base of the dolomitic marker2 D2 of Hettangian age and regional extension. Palynological dating enables us to assess the age of Triassic deposits from Lower Carnian to Rhetian.

In the Oued M'ya basin, the Triassic is subdivided into six lithological units, from bottom to top: the lower series, the eruptive rocks, the T1 level (Reservoir C and B), the T2 level (Reservoir A), the lower clay and the SaliferousS4. The topography of the Hercynian unconformity surface and the extensional tectonic regime during Triassic rift activity are the major factors controlling the distribution of Triassic sediments. Triassic sediments were deposited in semi-arid to arid climates over a wide area, in the form of fluvial valley-fill deposits. The lower series levels, T1 “B & C” and T2 “A”, are the main reservoirs in the basin (Table 02 SONATRACH and SCHLUMBERGER, 2007).

Source rock

The main source rock for the Triassic reservoirs in the Oued M'ya basin is the Silurian radioactive clays. The Ordovician clays (El Gassi clay and Azzel clay) are secondary source rocks. The reservoirs are supplied with hydrocarbons by vertical migration along faults and/or by lateral migration along permeable drains.

Reservoirs

Lower series

This represents the base term of the Trias and is the main reservoir in the central part of the depression (block 438). It is represented by alternating brown to green silty clays and white, reddish-brown to greenish, fine to coarse, conglomeratic sandstones. In the areas closest to the sources of supply, the detrital material is coarser with abundant conglomerates (Benkahla, Haoud Berkaoui, Gar and Echouf, Guellala areas), with thin intercalated clay banks. They were deposited in a fluvial environment with a braided network, originating from the Hassi Messaoud and Tilrhemt-HassiR'mel poles, evolving towards the north towards meandriform deposits, with a marine influence that is felt through increasingly carbonated levels. The total thickness of the lower series averages 50 to 70 m (varying from 0 m to more than 90 m).

Reservoir quality in this unit is largely controlled by sedimentary facies and their textural characteristics. Grain size and levels of cement and binders are the main factors controlling permeability. The sandstones of the lower series have been subjected to the effects of intense diagenetic activity in the north of the basin. Pressure-dissolution and the formation of feeder quartz are common. Anhydrite, carbonate and salt cements are also present.

Average porosities in the lower series are 9 to 12% and permeabilities can exceed 100 mD.

T1 and T2 levels

These levels are represented by fine to coarse brownish-red sandstones and brownish-red silty, slightly dolomitic clays. Their sedimentation, like that of the lower series, is characterised by an increase in subsidence and thickness towards the NE. This is controlled by the new relief created by the emplacement of eruptive deposits and tectonic replay linked to the activity of the Triassic rift. Units T1 and T2 were deposited in a fluvial continental environment, gradually shifting NEwards to fluvio-deltaic sedimentation. Correlation sdiagraphiques show a superposition of several sequences corresponding to channel deposits or point bars. The sandstones are grey and red micaceous, coarse at the base or with clay pebbles.

The sequences are separated by banks of reddish-brown or grey-green floodplain clay, with the presence of palaeosols. The total thickness of the T1-T2 units averages around 100 m, increasing towards the north, where it can exceed 200 m.

The average porosity of T1 and T2 reservoirs is 15-20%, and average permeabilities are greater than 200 mD.

Source rock	Radioactive Silurian clay (primary); El Gassi clay and Azzel clay (secondary)
Seals rock	Provided on a regional scale by the thick evaporitic series of the S4 saliferous Triassic and the S3 to S1 levels of the Lias. The clays interspersed between the Triassic reservoirs may constitute local cover. When they are thick enough and not fractured, the eruptive rocks provide good local cover for the reservoir Lower series
Traps	Structural type (low amplitude structures), mixed (case of the Benkahla structure) or purely stratigraphic (bevel and bar point Reservoirs in the lower series and T1)

Table 02: Source rock, Seal rock and trap type in the Triassic (SONATRACH and SCHLUMBERGER, 2007

I.1.4. Evaluation of Block 438

This corresponds to the western part of the Algerian Triassic Basin and represents the most explored area of this basin. This area is located between the two deposits of Hassi R'mel to the northwest and Hassi Messaoud to the southeast (Figure 6).

This block extends over approximately 400 km in longitude and 300 km in latitude, covering an area of approximately 120,000 km2. The Paleozoic and Triassic targets are located at a significant depth, between 3,400 m and 4,000 m.

Within the Triassic, the primary target is the lower series, while the T1 reservoir is a secondary target over a large portion of the block.

The Lower Devonian is present only along the axis of the Oued M'ya Trench, and the Ordovician targets are practically marginal and of little interest

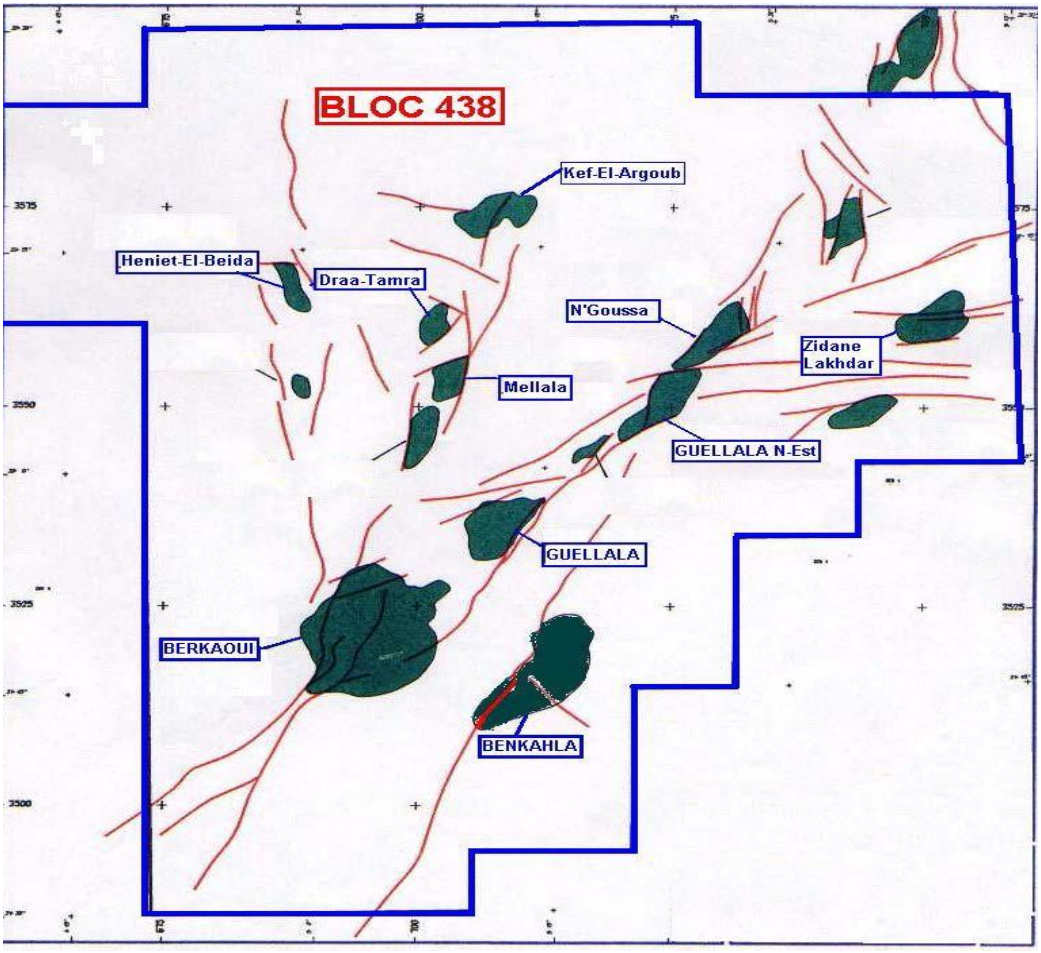

Figure 06: Map of the main accumulations in block 438BEICIP(BEICIP,1992).

From a structural point of view, with the exception of the Haoud Berkaoui structure, which has a vertical closure of around 300 m, this area is generally poorly structured. This, combined with the presence of thick evaporitic series within the Mesozoic overburden, makes it very difficult to define structural traps using seismic. The definition of these low-amplitude closures is also greatly influenced by the significant variations in velocity, which are partly linked to the complex distribution of the saliferous Senonian.

The structures revealed are organised along fault-related trends, mainly oriented north-south and north-east/south-west, the most important of which corresponds to the axis of the Oued M'ya trench (Haoud Berkaoui/ Guellala/Boukhezna-Sahane trend). These trends are intersected by transverse east-west trends, which acted as a late-stage fault.

Most of the structures have been drilled and correspond to:

The three deposits of Haoud Berkaoui, Guellala and Ben Kahla developed in the lower series.

The other accumulations developed in the block, and a multitude of peripheral fields which are, in order of importance: N'Goussa, Guellalanord est, Draa Tamra and Mokh El Kebechs.

I.2 Local context: presentation of the Benkahla field

I.2.1. Geographical location of the Benkahla deposit

The Benkahla field is located in the region formerly known as Gara Krima, about 80 km west of Hassi Messaoud, about 20 km south of the Guellala field and the same distance east of Haoud Berkaoui. It covers an area of around 83.5 km2 (Figure 07)

The Benkahla zone is located in the wilaya of Ouargla, between the two regions of Hassi Messaoud and HassiR'Mel, 600 km south of Algiers.

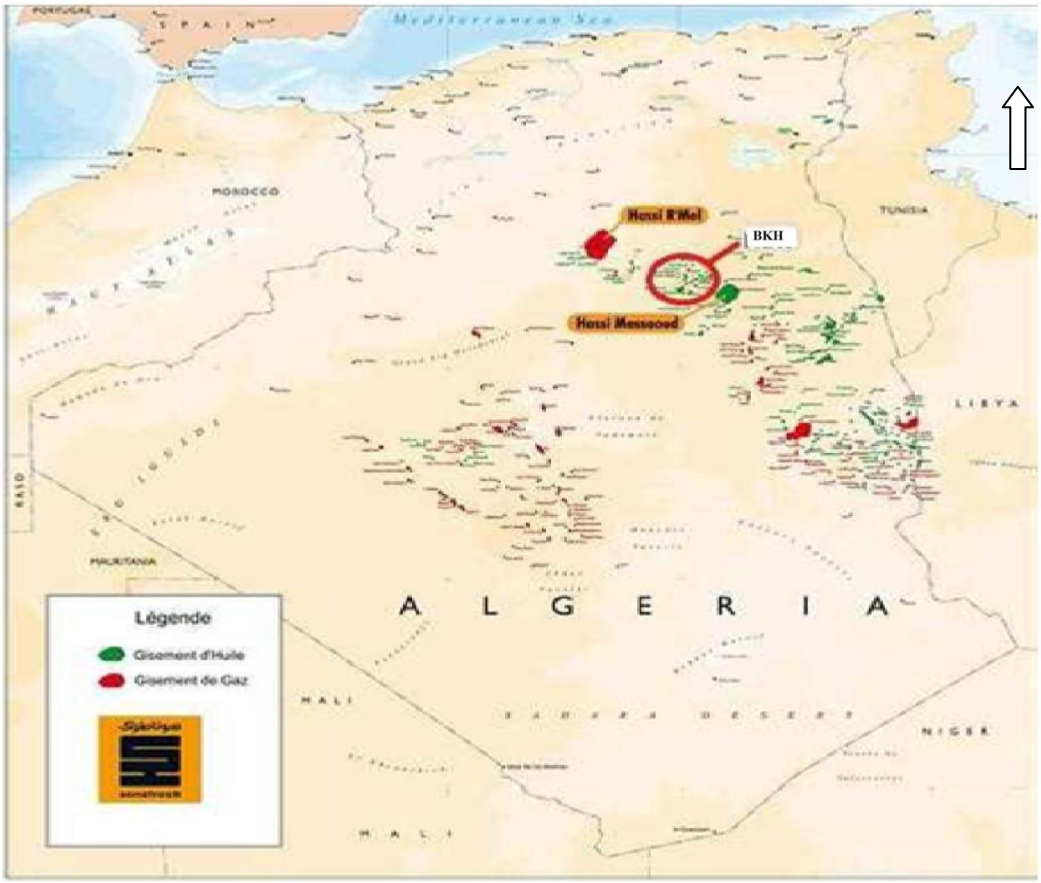

Figure 07: Geographical location of Bentalha. (SONATRACH/ EXPLOTATION,1995).

I.2.2. Geological setting of the Benkahla deposit

The Benkahla deposit is located in the Oued M'ya depression, in the centre of the Triassic province, where it is bordered to the west by the HassiR'Mel field, to the north-west by the Berkaoui deposit, to the north-east by the Galalla deposit, to the east by the Hassi Messaoud field, and to the south by the El-Gassi deposit.

I.2.3. History of the study area

The Haoud Berkaoui regional office is located in the commune of Rouissat, 25 km from the capital of the wilaya of Ouargla. The region was managed by Hassi Messaoud until 1977, when it became autonomous.

Geophysical studies carried out in the Ouargla region have revealed the existence of two (02) structures called: Haoud Berkaouiet Benkahla, both located on a surface area of 1600 km².

The first hole drilled in the Ouargla region in 1963 was OA01. In March 1965, the French petroleum company CFPA drilled the first hole, OK101, at the top of the Haoud Berkaoui structure, locating an accumulation of light oil with a density of 43°API (d = 0.8) in the lower Triassic clay-sandstone series (TAG). This borehole reached the Gothlandian at 3327.8 m (the first Palaeozoic horizon encountered beneath the Hercynian unconformity). Following this drilling and seismic interpretations, a second OKP24 well was drilled on: 31/08/1966 in the Benkahla structure, where it also encountered oil in the T.A.G. To evaluate this new structure another well OKS55 was drilled.

The production test carried out by CFPA gave a flow rate of 11 m3/h with a reservoir pressure of 520 kg/cm2 and a GOR of 101 m3/m3. This successful test was promising, and persuaded the producers to install other wells in the vicinity of the structure, which helped identify other peripheral deposits.

To date, 38 wells are in operation, spread across all the fields, including 27 producing wells and 08 water injector wells to maintain pressure. The other 03 wells are dry wells.

All the oil and gas recovered is sent to the various production centres in the region. The main activities in the region are:

* Oil and condensate production;

* Production of associated gas (sales gas and lift gas);

* Water injection.

I.2.4. Benkahla stratigraphic column

From a stratigraphic point of view, the distinctive feature of the Triassic province is that the Mesozoic rests in a Hercynian unconformity on the Palaeozoic (Figure 08). This allows us to point out that the Benkahla area has three entire sub-systems which have been eroded:

- The Devonian;
- The Carboniferous;
- The Permian.

The stratigraphy starting from the Palaeozoic is as follows:

II.1.4.1. The Paleozoic

The stratigraphic data obtained from 32 boreholes at the deposit in this period are Silurian.

A. The Silurian

This stratigraphic unit, formerly known as the Gothlandian, was greatly affected by the Hercynian unconformity. It is composed of black, flaky, carbonaceous clays, sometimes carbonated, becoming very fossiliferous at the top, with sandstone intercalations sometimes a few metres thick.

II.1.4.2. The Mesozoic

The Mesozoic is well developed in the Triassic province.

A. The Triassic

It is composed of a sandy-clay series of continental origin resting unconformably on the various terms of the Palaeozoic and ends in a salty-clay series of lagoon-marine origin, which constitutes an excellent cover for the deposits of the sandy Triassic, and is composed from bottom to top:

*** The Lower Series**

This is the main reservoir in the Haoud Berkaoui and Guellala fields, but the only reservoir at Benkahla. (Sonatrach/ EP) This geological series, made up of clays and sandstones, is unconformable with the Silurian (Hercynian unconformity) and is also covered by andesitic deposits. Its average thickness is around 40 to 50 m, consisting of a succession of coarse

sandstones, fine to medium sandstones, very fine sandstones and frequently dolomitic clay (J.Thouvenienjan 1968).

These different constituents are generally arranged in sedimentary sequences, ranging from the course at the base to the finest at the top.

These clays are sometimes green at the top, sometimes grey. The intercalations of the clay joints are grey-green in the order of centimetres, and are finely laminated.

Less flattened pebbles are sometimes encountered, the probable cause being a sequential cessation of mud deposition. Towards the base, brown-red clays, sometimes brecciated sandstone and soft pebbles were deposited, with frequent concretions of pink dolomite.

***The eruptive series (Andesitic series)**

This is a series of volcanic outpourings within the lower series or towards the end of its sedimentation. Its thickness varies from 0 to 70 metres at Haoud Berkaoui, averaging 130 to 140 m at Guellala, and 0 to 80 m at Benkahla.

This series is sometimes interspersed with dolomitic or silty red clays (OKS30, OKS32 and OKS35).

Its thickness increases from south to north of Benkahla. The presence of intra-andesite sandstone intercalations, containing a pressure higher than that of the reservoir, seems to show that the eruptive forms the cover of the Benkaha deposit. A test carried out at the top of an intra-andesite detritic level at OKS30 recovered salt water at 320g/l. The virgin pressure was 477Kg/cm2, while the pressure in the lower series was 210Kg/cm2.

Above the Andesite and in the southern part of Benkahla, there is a past of kinerite clay varying in thickness from 1 to 6 metres. However, some boreholes have not encountered the Andesite Series. According to J-Thouveninjan 1968, kinerite clays are the only manifestation of volcanism (PL2). These kinerite clays form a ferruginous armour (Paleosol).

*** Sandstone Triassic T1**

This formation is a sandstone-clay sequence varying in thickness from 20 to 30 metres. At the top, there is a bank of dolomitic and brecciated clay about 10 m high. The T1 level was deposited throughout the Haoud Berkaoui and Guellala region, except at Benkahla, where it is very thinly deposited.

The presence of this weak deposit to the south of Benkahla leads us to believe that these deposits were interrupted by a volcanic phenomenon, or else the structure was much higher at the time of sedimentation. T1 can be subdivided into two sub-layers:

- A clayey-dolomitic sub-layer at the top, around 8m thick;

- A sandstone sub-layer, 12m thick.

*** T2 Triassic sandstone**

At the top, there is a reddish-brown silty-clay sub-layer, around ten metres thick. It is dolomitic with fissures filled with salt and anhydrite. A sandstone sub-layer lies at the base (medium to fine grained from 8 to 10 m).

B.The Jurassic

This is made up of evaporitic (lagoon-marine) deposits, with a thickness of around 850m, and is subdivided as follows:

***The Lias**

Its thickness is around 340m-350m, subdivided into two lithological zones:

-At the base: massive salt (80m);

-At the top: massive anhydrite (260-270m).

The Jurassic wall is taken from the base of the marly bed, known as the "B" horizon, which forms a regional diagonal marker.

***The Dogger**

It is subdivided into two series:

1.The Dogger lagoon

It is 120 m thick and consists of alternating grey-green and brown-red clays, grey marl and anhydrite.

2.The clayey Dogger

This series is made up of plastic clays and indurated clays, grey marls that are sometimes dolomitic and intercalations of fine sandstones.

***The Malm**

This is a clay-sandstone-limestone complex 234 m thick, composed of alternating plastic clay, often silty, clay-dolomitic limestone and grey marl with gradations of intercalation.

C.The Cretaceous

***The Neocomian**

is composed of red brown clays and grey marls, often dolomitic with intercalations of fine sandstone and dolomitic limestone, 181m thick.

***Barremian**

This is made up of fine to very coarse sand and fine beige to brown-red sandstone, with some interlayers of brown-red silty clay and clayey limestone, 372m thick.

***The Aptian**

This is a carbonate, dolomitic microcrystalline series about 20 to 30 metres thick.

***The Albian**

This is a series of sandstones and clays with some dolomitic intercalations and alternating marl and clay at the top of the layer. It is approximately 460m thick.

***The Cenomanian**

161m thick, composed at the top of alternating white anhydrite, limestone, dolomitic marl and grey clay, and at the base of grey clay and dolomitic marl, with layers of dolomitic limestone, grey-green clay and brown-red clay.

***The Turonian**

is a series of marine deposits 70 m thick, made up of beige to white chalky limestone, with layers of clayey and dolomitic limestone at the top.

***The Senonian**

It is subdivided into:

1.The saliferous Senonian

It is formed of massive translucent salt with intercalations of hard crystalline anhydrite, soft grey clay, slightly dolomitic and saliferous, and at the base, it consists of massive anhydrite 220 m thick.

2.Anhydritic Senonian

This consists of alternating microcrystalline white anhydrite, sometimes crystalline, grey dolomite, beige limestone and brown-red dolomitic clay, 250m thick.

3.The carbonate Senonian

This has been affected by erosion and is marked by the Alpine unconformity at the summit. It is a carbonate series of white fossiliferous limestone, often dolomitic and vacuolated, with marl layers 225 m thick.

II.6.4.3. The Cenozoic

Only the Mid-Pliocene represents the Cenozoic terrain in the region, resting unconformably on the Mesozoic; its thickness varies from 30 to 70 m. It is made up of fine, coarse, sub-angular to rounded yellow sand, with layers of fine to medium sandstone, friable with carbonate cement and soft white limestone, sometimes dolomitic sandstone.

ÈRE	SYST	ÉTAGES		DESCRIPTION	EPAISSEUR
CENO-ZOIQUE		MIO-PLIOCÈNE discordance alpine		Sable, grès et argile	0 à 60 m
MESOZOIQUE	CRÉTACÉ	SÉNONIEN	CARBONATÉ	Calcaire dolomitique et marne	0 à 700 m
			ANHYDRITIQUE	Anhydrite massive,calcaire, dolomie, argile et marne	
			SALIFÈRE	Sel massif, anhydrite et argile	
		TURONIEN		Calcaire crayeux	
		CÉNOMANIEN		Argile grise, anhydrite blanche, dolomie et marne	
		ALBIEN		Grès fins à moyen à intercalations d'argile brun-rouge et de sable grossier à la base	300 à 900 m
		APTIEN		Dolomie et marne	10 à 30 m
		BARRÉMIEN		Sable fin à très grossier Passées de dolomie Calcaire et marne	600 à 1300m
		NÉOCOMIEN		Grès fins à moyen Passées d'argile et d'anhydrite, lignite	
	JURASSIQUE	MALM		Argile silteuse à intercalations de dolomie, de calcaire et de marne	120 à 300 m
		DOGGER	ARGILEUX	Argile indurée	
			LAGUNAIRE	Anhydrite et dolomie Passées d'argile silteuse	
		LIAS	ANHYDRITIQUE	Anhydrite massive blanche, intercalations de dolomie et argile	700 à 900 m
			SALIFÈRE	Sel massif incolore à rosé avec intercalations d'argile plastique	
			HORIZON "B"	Marne, argile dolomitique	
			S1 + S2	Sel massif incolore à rosé avec intercalations d'argile plastique	
			S3	Sel massif incolore avec intercalations d'argile plastique	
			ARGILES SUPÉRIEURES	Argile plastique salifère	
	TRIAS	S4		Argile brun-rouge parfois salifère	100 à 250 m
		ARGILES INFÉRIEURES		Argile silteuse	
		T2		Grès fin argilo-silteux	
		T1		Grès argileux	
		ROCHES ÉRUPTIVES		Andésite altérée	
		SÉRIE INFERIEURE discordance hercynienne		Grès fin à moyen	
	GOTHLANDIEN			Argile noire grés fin à moyen	300 à 900 m

Figure 08: Typical stratigraphic column at Benkahla (Production Division/ SONATRACH document).

I.2.5. Structure of the Benkahla deposit

I.2.5.1. Source rocks

The importance of the lower Palaeozoic series is linked to the presence of the basin's source rocks, the richest of which are the Silurian radioactive clays (Figure 11). In conjunction with the sedimentary condensation of the entire Silurian in this basin, these clays have excellent geochemical characteristics. Their shallow burial during the Paleozoic preserved their petroleum potential, with maturation and hydrocarbon generation taking place during their subsequent evolution under the influence of Mesozoic subsidence. Silurian bedrock is absent from the Hassi Messaoud and Talemzane clusters.

In the Oued M'ya depression, the Silurian bedrock is currently mature enough to generate oil. It is more mature (gas zone) to the west of HassiR'Mel and to the north of the Talemzane mole, where it becomes more deeply buried towards the South Atlasian Trench.

The current configuration of the basin and the extension of the Silurian bedrock have been extremely favourable for feeding the overlying reservoirs (Triassic and locally Lower Devonian) in the Oued M'ya depression.

In the west, the HassiR'Mel deposit, in the immediate vicinity of the Silurian wedge, was able to be fed, given its very favourable structural configuration. (Document Production Division/ SONATRACH). (Figure 09, 10)

I.2.5.2. Reservoir rocks

With the exception of a few reservoir levels located in the Lower Devonian at the heart of the Oued M'ya furrow, the Paleozoic reservoirs are limited to Cambro-Ordovician sandstones. These reservoirs are generally of poor quality, especially in the M'Kratta slab and the Hamra Quartzites. The extension of the latter is limited to the eastern part of the basin, where it is much thinner than on the western edge of the Berkine basin.

The most important reservoirs are those of the Cambrian, which are present throughout the basin. However, in areas where the Cambrian is covered by the Ordovician clay-sandstone series, it is generally very deep and in an unfavourable position relative to the source rocks. On the Talemzane mole, where it is partially eroded beneath Triassic sandstones, it is not covered.

On the other hand, on the El Agreb-Hassi Messaoud mole, the Cambrian cover can be provided by the clay facies of the Triassic, as the good reservoir levels were not deposited in this sector.

In the Oued M'ya depression, the Triassic reservoirs are similar, but the distribution of the reservoirs and their quality vary significantly, and we can distinguish (Document Division Production/ SONATRACH) (Figure 09, 10):

The lower series:

This is underlain by Palaeozoic bedrock, the best facies of which are found in the Oued M'ya depression, probably in connection with the Hassi Messaoud palaeomole. This series is the main reservoir for the Benkahla, Guellala and Haoud-Berkaoui deposits, as well as a large part of block 438. This formation is considered to be equivalent to the Lower Clay-Sandstone Triassic (TAG) of the Berkine Basin.

Unit T1

In which some very interesting reservoirs have been developed in the western part of the basin (reservoirs B and C). On the other hand, in the Oued M'ya trench, the reservoir levels of this unit are greatly reduced (T1 reservoir) above a highly developed eruptive series in this sector, related to the distensional play of the major structural trends. This unit is equivalent to the carbonated Triassic of the Berkine basin and the intermediate Triassic reservoirs of the Rourde Nouss region.

Unit T2

, in which the 'A' reservoir is developed. This reservoir is particularly important in the HassiR'Mel field, but has been rapidly degraded elsewhere, in particular by widespread saliferous cementation on block 438.

This unit is equivalent to the Upper Clay-Sandstone Triassic (TAGS), which is at its most developed in the Rhourde-Nouss region.

I.2.5.3. Cover rocks

The evaporitic series deposited at the end of the Triassic through the Benkahla field constitutes an excellent regional cover over the entire Triassic basin. This cover consists of salts and anhydrites with thicknesses exceeding a thousand metres.

In addition to this regional coverage, there is local coverage specific to this reservoir. The Triassic eruptive rocks, which are well developed, originate from fairly large lava flows and play an important role in ensuring a good seal between the lower series and T2 (Figure 11).

The lower series reservoir is a litho-stratigraphic wedge-shaped trap bounded to the west by a regional fault that forms a screen and wedge to the south (Production Division/ SONATRACH document).

I.2.5.4. Migration

The hydrocarbons generated, especially in the northeastern part of the Oued M'ya basin, the most subsided part, migrated towards the high areas where the trapping took place. The migration took place from west to Hassi Messaoud, and from north to south in the direction of Haoud Berkaoui, Benkahla, Guellala and even Hassi Messaoud.

The timing between the establishment of the saliferous cover at the end of the Triassic and beginning of the Jurassic, and the start of hydrocarbon generation in the Middle Cretaceous, implies that all the hydrocarbons generated are accumulated and trapped in this same basin in the absence of leaks. (Document Production Division/ SONATRACH).

(Scale: H: 1:500 00, V: 1:2000 m)

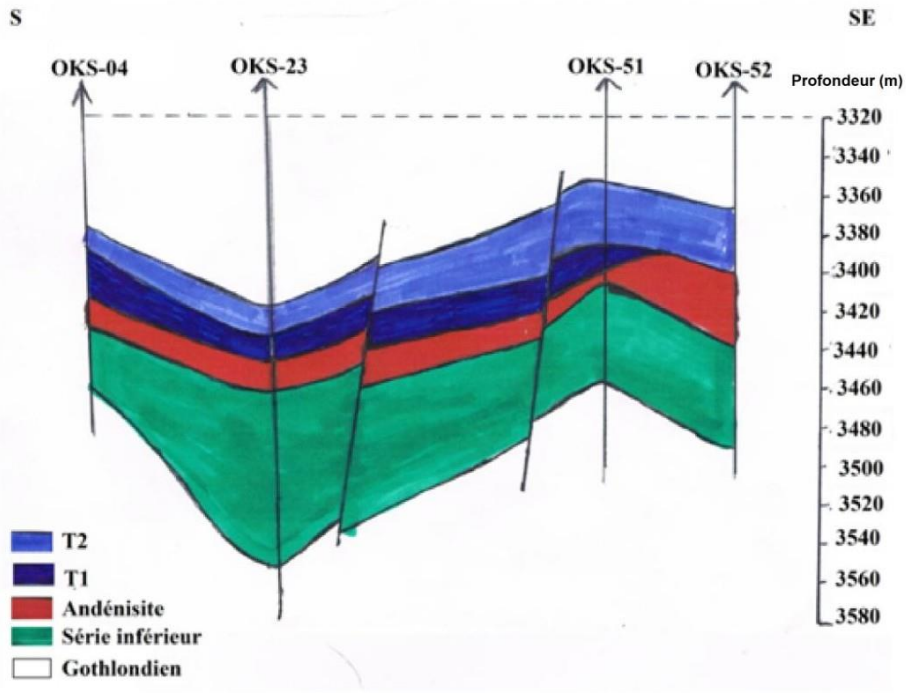

Figure 09: Geological section S-SE.(Nassira Mebrouki .2015.p30)

(Scale: H: 1/ 500 00, V: 1/ 2000m)

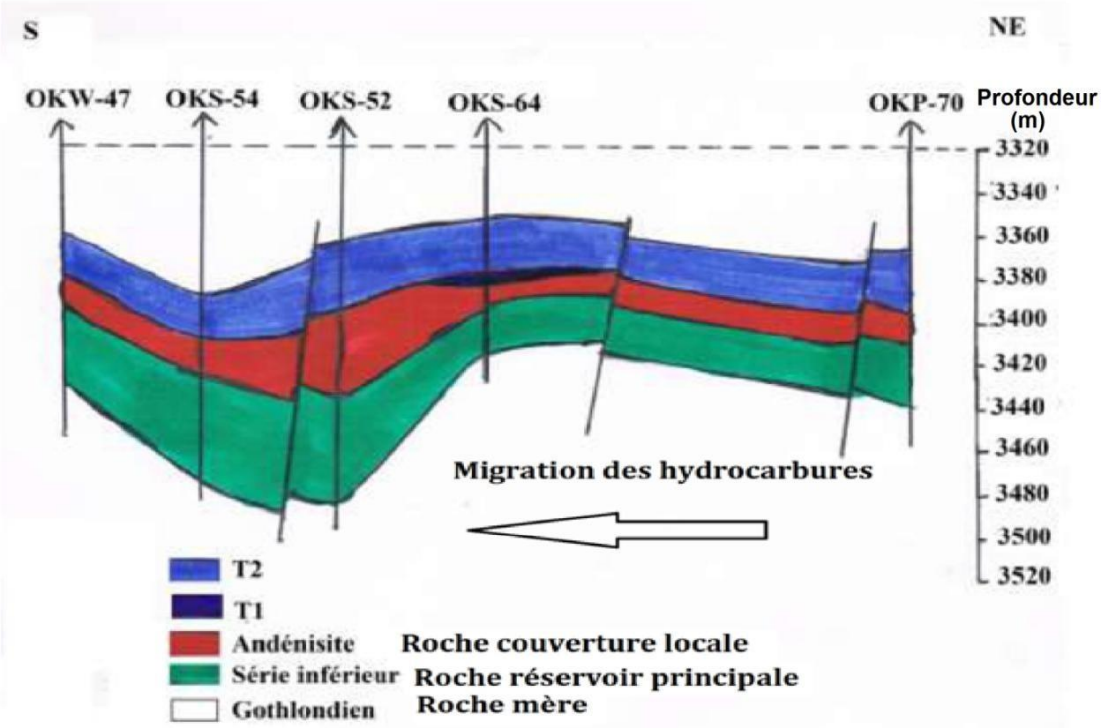

Figure 10: The S-NE geological section(Nassira Mebrouki .2015.p30)

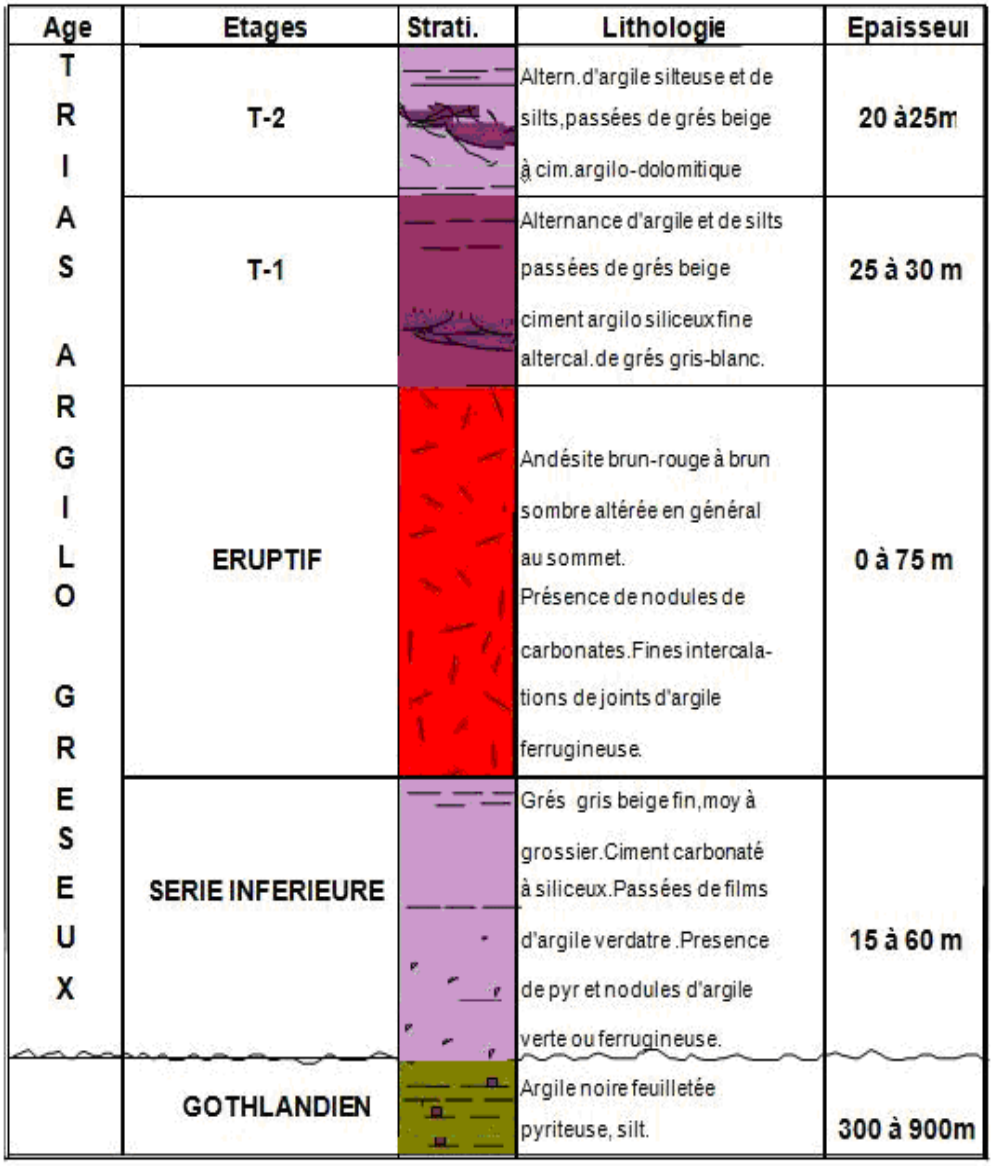

Figure 11: Stratigraphic section of the Triassic clay-sandstone (Production Division/SONATRACH).

Exploration efforts in the Oued M'ya basin have gathered momentum over the past five years, culminating in several oil discoveries. Particular interest has been focused on the possibility of extending the Triassic deposits, notably Berkaoui and Benkahla, and on developing the network of open fractures in the deep targets (Hamra quartzites: Ordovician). Several recent discoveries have been made in the basin:

- An oil deposit, Benkahla est, was discovered in the lower series reservoir (Trias) to the east of the Benkahla deposit (BKHE-1 well, 1999);

- An oil discovery in the Ordovician Hamra quartzite reservoir in the Berkaoui region (BKP-1 well, 2002);

- An oil discovery in the Triassic T1 reservoirs and lower series to the west of the Berkaoui deposit (BKO-1 to 3 wells, drilled between 2001 and 2005);

- Two oil discoveries, between the Berkaoui and Benkahla fields and to the north of Berkaoui, in the lower series reservoir (BKRE-1 well, 2005), and the Hamra quartzite reservoir (NHN-1 well, 2005).

Modelling and geochemical balances in the Oued M'ya basin show that a very large volume of hydrocarbons (around 3 to 4 times the total covered to date) remains to be discovered in different types of traps (structural, mixed stratigraphic, reservoir extensions and deep targets).

Chapter II : Method of working

Introduction

The process of core analysis provides vital information unavailable from either wire line log mesurément or drill cutting samples the amount of sedimentological information that can be obtained from a core is several orders of magnitude greater than is provided by wire line logs and cutting samples these types of information include detailed lithology, macroscopic and microscopic definitions of the heterogeneities of the reservoir rocks as well as basic reservoir data. Core data is also used to calibrate the log responses (Miall, 1984). The type of cores analyzed here in this study is conventional core in this study core from 10 wells (figure03.1) were examined, described and photographed as well as further core analysis and thin sections from these cores were carried out.

1. Technique and available data

1.1. Sampling method

• Cylindrical rock samples of diameter 2.54 cm and length 40 mm are taken at the core preparation and processing department of the

• Département Carothèque Centrale (DLCC) / HASSI MESSAOUD, in collaboration with the Service Pétro-physique.

• A sample shipping record is issued to the Reservoir Rocks Department after each end of the operation, in which:

• Well names

• Sample numbers per core;

• The carrot number(s);

• Name of operator(s);

• The date of the sampling operation;

• Carrot intervals

• region, basin, reservoir age, number of cores, and recovery rate.

• Lubricant type (Saturated Salt Water, Nitrogen, Diesel) ;

• Before starting the Soxhlets distillation process, samples should be checked and then stored in plastic boxes with information sheets from each stored well, prior to the washing process.

• Before acknowledging receipt, the technician must first ensure that the planimetry, sample numbers, core numbers, size, condition and nature of the samples (compact, friable, broken or deteriorated, sandstone, clay, carbonates, etc.) do not represent any anomalies likely to generate errors in the evaluation of petro-physical parameters of rocks.

1.2. Test methode

1.2.1. Equipment and Accessories

There are various techniques and methods of sample washing, the most frequently used of which is the Soxhlet distillation method. Solvents that are frequently used to extract hydrocarbons from rock pores are listed in the Appendix…, some are chosen for specific applications e.g., chloroform which is considered an excellent medium for crude oils and Toluene for crude and bituminous components. (Sonatrach document)

1.2.2. Purpose and scope

Before carrying out the porosity and permeability measurements, the original fluids contained in the pores of the samples, must be completely extracted from the pores. It is usually accomplished by means of using solvents to extract oil water and brine using Soxhlet's. (Sonatrach document)

1.2.3. Principle

Soxhlet extraction is the method usually used for washing core samples and is now frequently used by most laboratories. (Annex …), the solvent is brought to a slow boil in a pyrex flask, the vapours move upwards and the samples will be engulfed by the solvent vapours at an approximate temperature of 110°C. The water from the rock contained in the thimble will be vaporized. The solvent and water enter together in the inner chamber of the chiller, the cold water circulating in the inner chamber of the chiller condenses the water vapors and solvent into immiscible liquids. Decondensed solvents and water fall from the base of the chiller and overflow onto the samples. The solvent soaks the samples and

dissolves the oil with which it comes into contact. When the liquid level reaches the top of the siphon tube, the liquid in the siphon tube is automatically emptied by the siphon effect and flows into the balloon. The solvent is then ready to start another cycle.

Full extraction may last from several days to several weeks in the case of crude oil or the presence of low-density heavy residual hydrocarbon deposits. Low permeability samples, on the other hand, require a long-term extraction operation. (Sonatrach document)

1.2.4. Identification of samples

• The operator performing the Wash opération must first check the Following:

Samples intended for washing, with the exception of lithological facies such as shales and clays, must be taken from sandstone and carbonate levels;

The plugging of the samples must be directed in the direction of the flow of the Fluids;

The samples shall be shaped so as to obtain suitable sizes allowing the operator to easily place them in the cell of the measuring equipment. (Sonatrach document)

1.3. Core Analysis Data

For the petrophysical study, helium porosity and nitrogen permeability data 5108 side wall plugs are available. They are cored systematically each 15 cm of the cored intervals of nine wells (82 plugs from 3380.03-3408.57 m cored interval of OKS30 well; 32 plugs from 33887.91-3428.75 m interval of OKS32well; 104 plugs from 3356.28-3410.61 m interval of OS35 well;

78 plugs from 3369-3400 m interval of OKS39 well ; 86 plugs from 3457-3497 m interval of OKS40 well ; 62 plugs from 3447-3480 m interval of OKS42 well ; 52 plugs from 3427-3452m interval of OKS43well ; 106 plugs from 3487-3522 m interval of OKS44 well ; and 98 plugs from 3484-3517 m interval of OKS45well;122plugs from 3414-3453 m intrvel of OKS51well).These cored intervals cover all the T2, T1, Andésites , Série Inférieure, Gothlandien , units of the Cambrian reservoir sequence in Hassi Messaoud Field. The helium porosity is measured using the helium injection technique using the helium pycnometer at 16 psi, while the nitrogen permeability is measured using a nitrogen permeameter at 20-30 psi. The applied techniques are described and published in detail by many authors (Nabawy and Shehata, 2015;

Nabawy and Wassif, 2017; David et al., 2015; Nabawy, 2018; Abdeen et al. 2021; Baouche and Nabawy 2021; Abuamarah and Nabawy, 2021; Shehata et al., 2021; Fea et al., 2022; Haque et al., 2022; Fallah-Bagtash et al., 2022; Kassem et al., 2022). To decipher the reservoir quality of the Cambrian reservoir in Hassi Messaoud Field, the normalized porosity and reservoir quality indices (NPI in decimal & RQI in μm), the flow zone indicator (FZI in μm) of Amaefule et al. (1993), the effective pore radius R35 (in μm) of Winland (1972), and the discrete rock types DRT of Shenawi et al. (2007) were calculated based on the porosity (∅ in decimals) and permeability (k in mD) as follows.

$$NPI = \varnothing / (1 - \varnothing)$$

$$RQI2 = 0.000986 \times k/\varnothing$$

$$FZI = RQI/NPI$$ (Amaefule et al., 1993)

where ∅ in decimals, and k in mD.

$$Log\ R35 = (0.588 \times \log k) - (0.864 \times \log \varnothing) + 0.732$$ (Winland, 1972)

where ∅ in %, and k in mD.

$$DRT = ROUND(2 \times LN(FZI)+10.6,1)$$ (Shenawi et al2007)

This procedure and empirical equations were applied successfully by many authors to decipher the reservoir characteristics of various clastic and carbonate reservoirs (Nabawy and El Sharawy,2018; Nabawy et al.,

2020a,b; Abuamarah and Nabawy, 2021; Kurniawan et al., 2021; Safa et al., 2021; Radwan et al., 2021, 2022a, b; Fallah-Bagtash et al., 2022; Nabawy et al., 2022a; Ashoor et al., 2023; Elmahdy et al., 2023).

Chapter III: Petrophysical core and facies analysis

1. Lithological description of cores

1.1. Core OKS30 Well

Table 03: Lithological description of the Lower series of Core OKS30 Well

Depth	Lithological description	Floor
3380.4 to 3381.6m	Beige white sandstone with siliceous cement	Lower series
3381.6 to 3383.16m	Chocolate brown clays with passages of green silstones	
3383.16 to 3383.9 m	Fine to very fine beige white sandstone with siliceous cement become medium well classified with the presence of nodules dolomitic at the base	
3383.9 to 3384.65 m	Brown red clay	
3384.65 to 3386.5m	Fine to very fine beige white sandstone well classified	
3386.5 to 3388.15 m	Fine to medium beige white sandstone poorly classified	
3388.15 to3389.2 m	Chocolate brown clays with silty passages and sandstone	
3389.2 to3390.85 m	White beige sandstone sometimes fine to medium green grey sometimes coarse	
3391 to 3392.45 m	Hard, fine to very fine sandstone, green, rounded to sub rounded with siliceous cement, crossed by gallés of different nature become conglomeratic sandstone towards the base. No visual porosity medium to coarse cement	
3392.45 to3395.7 m	Green conglomeratic sandstone	
3395.7 to 3396.25 m	Grey to black clays, indurated and soft towards the base with films	
3396.25 to 3397.5 m	Fine green hard siliceous cement sandstone, well rounded, poorly classified with stratifications	

	horizontal to sub-horizontal rarely slightly oblique bituminous, low visual porosity	
3397.5 to 3398	3397.5 to 3398 Dark green hard, fine to medium siliceous cement sandstone, bituminous, rounded and poorly classified. Low visual porosity	Lower series
3398 to 3399.95	Hard, compact, fine to very fine green sandstone with cement carbonated, rounded, poorly classified, low visual porosity with presence of nodules of various natures	
3399.95 à 3401.8	Medium-green sandstones hard bituminous, rounded and poorly classified	

1.2. Core OKS32 well

Table:04 Lithological description of the Lower series of core OKS32

Depth	Lithological description	Floor
3387.30 to3388.10 m	Fine to very fine grey-black sandstone with siliceous cement, speckled with beige sandstone nodules.	Lower series
3388.10 to 3391.50 m	Soft reddish-brown clay becomes greyish indurated towards the base, with siliceous passages around 3390.80 m.	
3391.50 to 3391.70 m	Girès fine to very fine grey clay cement, cross-laminated	
3391.50 to3391.70 m	Fine to very fine compact hard gray sandstone	
3392 to 3392.70 m	Complex of grey clay and reddish fine sandstone and grey clay with silty indurations at base	
3392.70 to3394.10 m	Fine to very fine grey-black sandstone, slightly bituminous in places, compact with siliceous cement	

3394.10 to 3395.10 m	Soft grey clay.	
3395.10 to 3397.45 m	Grey-black, fine to very fine, slightly bituminous sandstone with siliceous cement, hard, rarely horizontal to Joblique stratification. Very bituminous level towards	
3397.45 to 3397.70 m	Passage d'argile grise. Grès gris-noir, fin à très fin, légèrement bitumineux à ciment siliceux, dur, rarement	
3397.70 to 3398.60 m	grès grey-black fine to very fine slightly bituminous	
33980.60 to 3400 m	fine to very fine silty grey-black sandstone with red clay nodules in places.	
3400 to 3403 m	Beige to white, coarse to medium, sometimes micro conglomeratic sandstone with carbonate cement, presence of gray clay nodules, poorly classified visual porosity: low. Becomes grayish-black, fine to very fine, slightly bituminous around 3402.50 m	
3403 to3403.20 m	Transition from fine sandstone to grey clay nodule	
3403.20 to 3403.50 m	fine to very fine grey-black sandstone, slightly bituminous	
3404 to3404.90 m	Grey to grey-black sandstone, fine to very fine, sometimes medium, slightly bituminous with various types of cement. Very bituminous level around 3404.75 to 3404.90 m	
3404.90 to 3407.45 m	White beige to grey-green sandstone, fine to medium, becoming medium to coarse with carbonate cement, Nodules of various types and sometimes conglomerates are present.	Lower series
3407.45 to 3407.75 m	indurated gray clay	
3407.75 to 3408 m	Fine to very fine grey-green sandstone with siliceous cement	
3408 to3408.60 m	Fine to medium-grained black bituminous sandstone with H to sub-horizontal stratification	
3408.60 to 3409.50 m	Grès gris, fin a moyen bien classé a stratification H à sub horizontale	
3409.50 to3411.30 m	Grey sandstone, fine to very fine, sometimes silty, becoming medium in places locally bituminous grey sandstone, rarely horizontally stratified. Grey clay nodules present at base. Sometimes micro conglomeratic sandstone	
3411.30 to 3413.60 m	Fine to grey-black, coarse to medium-grained, micro conglomeratic sandstone with carbonate cement, locally bituminous with cm passage of grey clay. Viscous porosity: low, rarely grey clay nodules.	
3413.60 to3415 m	Grey-green, fine to very fine, compact, hard sandstone with slightly carbonated cement.	

3415 to 3415.90 m	Grey-black sandstone, fine with ferruginous cement at base. passage of grey clay around 3415.80 m	
3415.90 to 3417 m	Medium to coarse grey to grey-green sandstone with locally carbonated cement, rarely grey clay nodules.	
3417.70 to 3418.50 m	Fine to medium-grained dark sandstone, slightly bituminous, rarely nodulated with grisc. clay.	
3418.50 to 3422.70 m	Coarse to medium grey-dark sandstone, frequently with grey clay nodules, becomes microconglomerated at 3421, often carbonated cement porosity: low moderately bituminous from 3422.30 to 3422.50 m	

1.3. Core OKS35 well

Table 05: Lithological description of the Lower series of Core OKS35

Depth	Lithological description	Floor
3365 à 3367.70 m	Fine to very fine clayey red-brown sandstone	Lower series
3367.70 à 3370.05 m	Light grey to medium beige sandstone to well consolidated with micro conglomeratic level and a few nodules of greenish clay.	
De 3370.05 à 3371.40.	Red-brown clay.	
3371.40 à 3376.40 m	Grey-beige to fine-beige sandstone becoming medium to coarse with numerous nodules and greenish clay inclusions	
3376.40 à 3378.6 m	Red-brown clay versi color.	
3378.6 à 3382.70 m.	base.Beige grey sandstone, fine light grey pfs fine speckled dark grey, medium to coarse with fine passed and nodules of greenish clay. Passage of gray clay at	
3382.70 à 3387.90 m.	Dark grey to black sandstone medium to coarse bituminous at intervals. Some greenish clay	
3387.90 à 3388.90 m	Red-brown clay	

3388.90 à 3392.65 m	Light grey sandstone, beige pfs black medium to coarse mottled bituminous towards the base	Lower series
3392.65 à 3399.35 m	Grey clay becoming brown red Intercalation of dcm of grey sandstone beige.	
3399.4-3402.4m	Medium to coarse-grained bituminous sandstone.	
3402.4-3405.3m	Grey clay, sometimes greenish, with a transition to medium to coarse grey sandstone.	

1.4. Core OKS 39 well

Table 06: Lithological description of the Lower series of core OKS 39

Depth	Lithological description	Floor
3369 to 3371.9 m	Light sandstone to beige, fine to medium well Consolidated with greenish clay towards the Base.	Lower series
3371.9 to 3373.7 m	Grey clay Sambre to brown sambre with passages of fine to very fine sambre sandstone.	
3373.7 to 3374.2 m	Grey clay sambre to brown sambre	
3374.2 to 3382.6 m	Grey sandstone Beige to white-grey, fine to Medium occasionally coarse Well consolidated with Interlayers andLight-grey clay nodules to greenish-grey.	
3386 to 3393.6 m	White sandstone To beige-grey becoming grey sambre to black-grey, medium to Bituminous coarse with Film and clay nodules Greenish. Conglomerate level Clayey sandstone. Grey clay. Bitumen. Passage of grey clay.	
3393.6 to 3395.9 m	Grey to beige-grey speckled sandstone, medium to coarse	

	with a small passage of grey clay	
3395.9 to 3396.7 m	Grey sandstone sambre to black, medium to coarse bituminous.	
3396.7 to 3397 m	Grey clay	
3397 to 3399.35 m	Grey sandstone light coarse to very coarse with micro conglomeratic passages, notably towards the base. Clay nodules. Micro conglomeratic passages.	
3399.35 to 3404.95 m	Grey clay Gradually turning black Piratized flaky clay	

1.5. Core OKS40 well

Table 07: Lithological description of the Lower series of core OKS40

Depth	Lithological description	Floor
3450 to 3461.5m	Reddish-brown clay with greening, with presence of clay carbonate and reddish-brown gres. Red-brown clay	Lower series
3458.5 to 3458.8m	Fine to medium reddish-brown gres	
3458.8 to3459m	Red-brown clay	
3459.5 to 3459.9m	Brown-red silty clay	
3459.9 to 3461.7m	Clay carbonate passage	
3461.7 to 3466.9m	Brownish red to light grey to beige, fine to very fine, well consolidated, compact, unobservable horizontal to subhrizontal stratification. Fine beige sandstone. Passage d'argile Gres brun rouge fin moyen stratification horizontale a subhorizontale. Clay-grey carbonate level composed of clay and nodules of gres and calcite.	
3466.9 to 3469.6m	Reddish-brown to greenish-grey indeure clay	
3469.6 to 3470.3m	Carbonates	
3469.6 to 3470.3m	Fine to medium beige to light-colored gres	
3470.8 to 3471m	Passge d'argileux conglomeratique	
3471 to 3472.4m	Red-brown clay	
3472.4 to 3473m	Fine to very fine clayey grey to grey verdate	

	sandstone	
3473 to 3475m	Medium gray to beige speckled gres	
3475 to 3475.5m	Medium to coarse gravel plain clay nodules	
3475.5 to 3476m	From gray clay to greenish gray	
3476.4 to 3477.58m	Medium beige gres with green clay nodules	
3478 to 3479.6m	Beige to light-grey medium-grained myennitment consolidated bituminous by endroite with clay nodules	
3479.6 to 3480.6	Gres plain clay nodules	
3480.6 to 3483.3m	Gresous conglomerated passage composed of medium to coarse light-grey sandstone with green clay pebbles and little to no consolidation.	
3483.3 to 3490m	Gresous conglomerated passage composed of medium to coarse light-grey sandstone with green clay pebbles and little to no consolidation.	
3490 to 3497.65	Light gray to beige sandstone, sometimes speckled, medium to coarse with streaks and some greenish clay nodules, horizontal to subhorizontal stratification. Covered sandstone, white films	

1.6. Core OKS42 well

Table 08: Lithological description of the Lower series of core OKS42

Depth	Lithological description	Floor
3447 to 3449.7	Grey to light beige fine compact sandstone with clay cement, presence of micro conglomerat. Dark speckled bituminous sandstone. Dark to medium-black bituminous sandstone, subhorizontal stratification. Dark to black speckled bituminous sandstone, with clay nodules	Lower series
3449.7 to 3450.1	Fine compact light beige sandstone presence of occasional clay.	
3450.1 to 3450.5	Dark to coarse black sandstone bituminous, horizontal stratification	
3450.5 to 3451.5	Grey to fine beige compact gravel, clay nodules.	
3451.5 to 3451.9	Medium dark sandstone, stratification criss-crossed	
3451.9 to 3452.1	Medium to coarse dark sandstone.	
3452.1 to3452.7	Dark to coarse black sandstone bituminous, stratification subhorizontal.	
3452.7 to 3453	Very fine grey compact sandstone, cement clay.	
3453 to 3453.8	Dark to medium to coarse black bituminous, stratified subhorizontal, nodules	

	of reddish-brown clay at the top. conglomerates, with sandstone and clay interlayers. Dark to black medium to coarse bituminous sandstone.	
3453.8 to 3459.4	Fine to medium-grained grey clay sandstone.	
3459.4 to3460.3	Reddish-brown clay, with greenish clay nodules.	
3460.3 to 3461.2	Silty clay with interlayers decimetric grey sandstone, presence pyrite.	
3461.2 to 3463.2	Silty clay with interlayers decimetric grey sandstone, presence pyrite.	
3463.2 to 3463.6	Silty grey clay.	
3463.6 to 3465.3	Medium grey to dark sandstone, horizontal stratification.	
3465.3 to 3469.6	Silty grey clay with centimetric intercalations of sandstone beds	
3469.6 to 3470.7	Compact fine grey to beige sandstone, horizontal stratification.	
3470.7 to 3471.6	Dark coarse-grained sandstone sub horizontal	
3471.6 to 3472.5	Beige silty clay	
3472.5 to 3473.7	Grey to beige silty clay.	
3473.7 to 3474.6	Gray to medium-dark subhorizontal. Bituminous	
3474.6 to 3479.6	Grey to dark coarse gravel bituminous	
3479.6 to 3480	Gré light grey medium	

1.7. Core OKS43 well

Table09 : Lithological description of the Lower series of Core OKS43

Depth	Lithological description	Floor
3427 to3429.7m	Sub-horizontal stratification in this area	
3429.7to3431.7m	Grey clay with intercalation of decimetric beige sandstone	
3431.7to3432m	Grey to dark medium bituminous sandstone	
3432to 3432.8m	Intercalation of beige sandstones and dark sandstones, with the presence of a centimetric clayey bed.	
3432.8 to 3432.9m	Medium dark bituminous sandstone	
3432.9to3433.6m	Medium dark sandstone with greenish nodules	
3433.6 to3435.1m	Dark to black sandstone with medium to coarse grain size	

3435.1to3435.5m	Grey to light beige sandstone with medium grain size	Lower series
3435.5 to3436.4m	Dark to medium black sandstone	
3436.4to3437.5m	Fine beige sandstone; Beige to medium to fine grey sandstone	
3437.5to 3437.7m	Dark to medium black sandstone	
3437.7to 3438.9m	Grey to greenish clay	
3438.9to3439m	A dark to black medium-grained centimetric sandstone bed	
3439 to3439.8m	Grey to greenish clay	
3439.8 to3439.9m	Dark to black medium-grained sandstone	
3439.9to3441.9m	Grey to greenish clay	
3441.9to3443m	Medium to coarse dark to black sandstone	
34433to443.6m	Medium to coarse dark to black sandstone	
3443.6 to3444m	Medium-light beige sandstone, presence of clay nodules	
3444 to3444. 3m	Medium to coarse dark to black sandstone	
3444.3 to3444.4m	Grey to light beige sandstone	
3444.4 to3445.9m	Dark to black medium to coarse bituminous sandstone	
3445.9 to3446.8m	Greenish-grey clay	
3446.8 to 3447.1m	Medium dark sandstone	
3447.1 to3447.6m	Greenish gray clay Medium to coarse beige sandstone	
3447.6 to3447.9m	Grey to greenish clay	
3447.9 to3451.7m	Dark to black bituminous sandstone with coarse grain size	

1.8. Core OKS44 well

Table 10 : Lithological description of the Lower series of core OKS44

Depth	Lithological description	Floor
3487to3487.4m	Greenish clay	
3487.4 to 3488.1m	Bituminous sandstone, medium to coarse	
3488.1to 3489.8m	Intercalated fine to medium grey sandstone, greenish clay	
3489.8to 3491.3m	Bituminous sandstone, with grey to grey-black clay in between	
3491.3to 3492.1m	Fine to medium dark grey sandstone	
3492.2to 3492.3m	Grey clay	
3492.3to3496m	Bituminous sandstone, fine to medium	
3496 to3496.6m	Dark gray to beige sandstone	
3496.6to3499m	Reddish-brown clay, sometimes greenish	
3499 to3501.3m	Medium to fine dark grey bituminous sandstone.	
3501.3to3501.4m	Passage of greenish clay	

3501.4 to3502.7m	Medium to fine dark grey bituminous sandstone	Lower series
3502.7to 3504.1m	Reddish brown to greenish clay with centimetric passage of beige sandstone	
3504.1to 3507m	Reddish brown to greenish clay with beige sandstone, fine	
3507to3512.4m	Fine to medium-grained beige to dark gray sandstone, with greenish clay nodules.	
3512.4to3512.7m	Passage of grey clay	
3512.7to 3514m	Fine to medium-grained beige to dark grey sandstone with greenish clay nodules	
3514to 3514.2m	Passage of grey-black clay, presence of pyr	
3514.2to 3517m	Dark grey to black bituminous sandstone	
3517to3522m	Alternating fine to very fine beige-grey sandstone with black clay.	

1.9. Core OKS45 well

Table 11: Lithological description of the Lower series of core OKS45

Depth	Lithological description	Floor
3484.10 to 3485 m	Fine to medium bituminous grey-black sandstone	Lower series
3485 to 3486.5 m	Dark grey, black, medium to coarse sandstone, poorly classified +/- hard, frequently bituminous, rarely conglomeratic	
De 3486.5 to 3487. 4 m	Grey-black sandstone, fine to medium, coarse pfs, poorly classified, bituminous, mottled	
3487.4 to 3487.9 m	Greenish silty clay	
3487.9 to 3489.90 m	Medium-hard, coarse to medium, to microconglomeratic, poorly graded, grey-black bituminous sandstone with interlocking to sub-horizontal stratum Presence of green clay nodules	
3489.90 to 3490.10 m	Greenish silty clay	
3490.10 to 3491 m	Grey-cliar to dark sandstone, mottled, fine to very fine +/- silty, crumbly, sub-horizontal stratum	
3491 to 3491.40 m:	Greenish silty clay	
3491.40 to3492.50 m	Light grey sandstone, clayey, fine to very fine silty, crumbly	
3492.50 to 3494.70 m	Dark grey sandstone, black pfs, bituminous, fine to very fine, moderately hard Start: oblique to sub-horizontal presence of nodules of various natures	
3494.70 to 3495.70 m	Greenish silty clay	

3495.70 to 3497.60 m	Grey-black sandstone, strongly bituminous, around 3496.2 to 3497.6 medium to coarse, poorly classified, moderately hard, knotty, mottled	
3497.60 to 3497.70 m	Passage of green clay	
3497.70 to3498.20 m	Conglomerate clay-sandstone complex	
3498.20 to 3501.20 m	Grey-black sandstone, bituminous, mottled, coarse to medium, poorly classified, microcongolomeratic, moderately hard	
3501.20 to 3501.40 m	Passage of green clay	
3501.40 to 3504.90 m	Dark-grey sandstone, coarse to 3502.8 m, fine to very fine, medium pfs to 3504.90 m mottled, knotty, horizental to sub-horizontal startification, hard, bituminous.	
3504.90 to 3506.30 m	Sandstone-clay complex: light-grey, coarse to medium sandstone, poorly classified, with very frequent green nodules	
3506.30 to 3512.2m	Dark gray, bituminous, medium to coarse sandstone, greenish clay intercalation, horizontal stratification. Black sandstone, bituminous, medium to coarse, with microconglomerates, greenish clay intercalation, horizontal stratification. Dark sandstone, bituminous, coarse, friable, with microconglomerates.	
3512.2 to 3517m	Light grey to beige sandstone, fine to very fine, compact, fissured	

2. Petrophysical Characters

The petrophysical characteristics of the Triassic sequence at Ben Kahla vary significantly from unit to unit in the SI of Units (SI) region, where the SI unit is also known as the lower sequence. The SI samples can be divided into six stable petrophysical reservoir types (PSRT1-6) (Table 01) in the ten wells studied (Table 01)

2.1. Static Petrophysical Reservoir Types (PSRTs)

The porosity and permeability values of the PSRT1 vary from 0.33 to 14.49 % (av. = 7.41%) and from 0.050 to 1590.7 mD (av. = 795.375mD), respectively. Thereby, its discrete rock type (DRT), RQI, FZI, and R35 values vary from 16.1 to 26 (av. = 21.05), 0.0992 to 7.4799 μm (av. = 3.78955 μm), 15.279 to 2248.5 μm (av. = 1131.8895 μm), and 89.738 to 16279 μm (av. = 8184.369 μm), respectively (Table 1). Based on the classification ranks of the reservoir quality

(Nabawy and El Saraway, 2018, Abuhagaza et al., 2021; Nabawy et al., 2022b; Elmahdy et al., 2023), the average rank of the RQI is good, while for the FZI, R35, and the RPI are vigorous and overestimated, so following the recommendation of Abuamarah and Nabawy (2021), they are described as fractures (Table 1). The PSRT1 has the best reservoir quality in the BON KAHELA, while the PSRT6 is characterized by the lowest quality. The porosity and permeability of the PSRT6 varies between 2.36 to 34.76 % of av. = 18.56%) and from 0.003 to 12.751 mD of av. = 6.377 mD, while its DRT, RQI, FZI and R35 vary from 4.7 to 11.6 of av. = 8.15, 0.241to 22.46 μm of av. = 11.3505 μm, 0.0536 to 1.237 μm of av. = 0.6453 μm, and 1.875 to 92.08 μm of av. = 46.36265 μm, respectively (Table 01). The average rank of the RQI, FZI, and RPI are tight, while for the R35 values are vigorous and overestimated, so they are described as fractures (Table 01): Petrophysical and reservoir quality data of the discriminated petrophysical static rock types (PSRTs) in BEN KAHELA Field, Algeria. The reservoir quality parameters are ranked following the classification ranks of Nabawy and El Sharawy (2018) and Radwan et al. (2022). where; DRT is the discrete rock type (Shenawi et al., 2007; Shehata et al., 2021), ∅ is the effective helium porosity, k is the measured permeability, R35 is the effective pore radius (Winland, 1972); RQI is the reservoir qulaity index; and FZI is the flow zone indicator (Nabawy and El Sharawy, 2018).

Table : Petrophysical and reservoir quality data of the discriminated petrophysical static rock types (PSRTs) in Benkahla Field, Algeria. The reservoir quality parameters are ranked following the classification ranks of Nabawy and El Sharawy (2018) and Radwan et al. (2022). where; DRT is the discrete rock type (Shenawi et al., 2007; Shehata et al., 2021), ∅ is the effective helium porosity, k is the measured permeability, R_{35} is the effective pore radius (Winland, 1972); RQI is the reservoir qulaity index; and FZI is the flow zone indicator (Nabawy and El Sharawy, 2018).

PSRTs	facies		DRT	∅%	k md	RQI µm	FZI µm	R_{35} µm
PSRT-1	Beige white sandstone with siliceous cemen	Min	16.1	0.33	0.050	0.0992	15.279	89.738
		Max	26	14.49	1590.7	7.4799	2248.5	16279
		Mean	21.05	7.41	795.8	3.78	1131.8	8184.3
PSRT-2	Grey sandstone medium, sometimes coarser	Min	15.1	1.25	0.194	0.1235	9.2545	90.445
		Max	16.0	18.02	957.88	2.4358	15.205	1541.3
		Mean	15.55	9.63	479.04	1.27	12.23	815.8
PSRT-3	Grey sandstone medium,	Min	13.1	0.78	0.011	0.0365	3.4446	24.583
		Max	15.0	19.09	544	1.7925	9.2483	1023.5
		Mean	14.05	9.93	272	0.91	6.34	524.04
PSRT-4	Grey sandstone medium,	Min	12.1	1.62	0.019	0.038	2.0725	22.469
		Max	13.0	22.63	121	0.7266	3.3596	327.08
		Mean	12.5	12.1	60.5	00.38	2.71	174.7
PSRT-5	Fine to very fine sandstone, sometimes medium	Min	11.1	1.26	0.008	0.025	1.2571	13.433
		Max	12.0	18.71	126.60	0.389	2.0633	169.26
	light grey compact hard sandstone with clay	Mean	11.5	9.98	63.3	0.20	1.66	45.6
PSRT-6	Grey clay becoming brown red Intercalation of dcm of grey sandstone	Min	4.7	2.36	0.003	0.241	0.0536	1.875
		Max	11.0	34.76	12.751	22.466	1.237	92.086
		Mean	7.8	18.5	6.3	11.3	0.6	46.9

2.2. Petrophysical characters of the different wells

The Triassic sequence is well represented in wells OKS30 and OKS51, located in the northwestern part of the Benkahla South Field (Table 01). However, the best reservoir quality

is observed in the SI unit at well OKS43, situated in the central northern area of the study zone (Table 01). Among the various wells, the sI unit consistently shows the most favorable reservoir properties, particularly at OKS43, where it demonstrates the highest reservoir quality (Table 01). Table 01 Petrophysical and reservoir quality data for the reservoir sequences in the studied wells of the Ben Kahla South Field, Algeria. Reservoir quality parameters are ranked according to the classification systems of Nabawy and El Sharawy (2018), and Radwan et al. (2022), considering the unit's name as SI

Well	Member		Depth	DRT	∅ %	k md	RQI µm	FZI µm	R_{35} µm	PSRTs
OKS35 Well	SI	Min	3356	4.7	2.64	0.007	0.0159	0.0535	1.9180	PSRT1-2
		Max	3410	18.9	34.76	1590.7	3.5121	67.298	4053.9	PSRT4-5
		Mean		12.3	6.33	9.24	0.23	3.44	131.0	PSRT4-5
OKS32 Well	SI	Min	3389	7.6	2.07	0.012	0.06	0.2235	4.637	PSRT1-2
		Max	3429	18.6	17	253.18	1.48	55.338	1357.5	PSRT5
		Mean		11.8	7.89	7.5	0.21	2.58	109.0	PSRT5-6
OKS30 Well	SI	Min	3380	7.4	2.18	0.010	0.0159	0.204	5.9467	PSRT1
		Max	3409	19.5	17.05	546	3.512	85.851	3336.3	PSRT5
		Mean		12.5	4.23	3.43	0.17	3.63	100.3	PSRT3,5
OKS39 Well	SI	Min	3369	9.8	0.87	0.011	0.03	0.66	23.117	PSRT1-2
		Max	3400	18.9	19.09	671.11	2.88	63.655	1618.1	PSRT6
		Mean		12.3	5.48	10.93	0.23	4.62	151.9	PSRT6
OKS40 Well	SI	Min	3457	5.8	1.9	0.003	0.0066	0.0912	1.817	PSRT1-2
		Max	3496	19.3	17.32	682.07	1.970	76.931	1683.2	PSRT5-6
		Mean		11.8	5.70	9.17	0.18	3.34	113.5	PSRT5-6
OKS42 Well	SI	Min	3447	8.1	1.41	0.09	0.0200	0.2812	7.295	PSRT1
		Max	3480	18.2	17	186.8	0.6479	44.380	1768.3	PSRT6
		Mean		12.1	6.10	8.38	0.22	3.32	125.2	PSRT5-6
OKS43 Well	SI	Min	3427	7.6	1.26	0.008	0.0163	0.246	5.687	PSRT1-2
		Max	3452	19	18.43	314.61	2.030	68.951	1937.7	PSRT3,6

		Mean		12.1	8.68	10.95	0.28	3.20	148.3	PSRT3,6
		Min	3387.19	6.3	1.29	0.018	0.016	0.115	**4.671**	PSRT2
OKS44 Well	**SI**	**Max**	3522	16.6	21.64	1087.7	2.720	19.909	**1819**	PSRT3
		Mean		13.3	2.14	1.01	0.10	9.33	**81.1**	PSRT3
		Min	3448.2	7.4	0.33	0.050	0.025	0.2021	**7.912**	PSRT2
OKS45 Well	**SI**	**Max**	3517.6	26	22.63	1040.8	7.479	2248.45	**1627**	PSRT4
		Mean		12.9	4.42	8.52	0.24	5.60	**159.89**	PSRT3-5
		Min	3414.03	6.7	3.62	0.015	0.01	0.14	**4.38**	PSRT1-2
OKS51 Well	**SI**	**Max**	3452.8	18.4	17.8	890	3.36	48.4	**2764**	PSRT3
		Mean		13.2	5.11	4.49	0.24	9.54	**183.6**	PSRT3

Table 12: Minimum, Maximum, and Average Values of Depth, Porosity, Permeability, RQI, FZI, and R35 for PSRT Units in OKS Wells(**Source: Excel, company documents**)

2.3. The significance of facies types on the classification of petrophysical reservoir rock types

Rock typing refers to summing up the benkahla reservoir samples into several static petrophysical rock types (PSRTs), each with its diagnostic petrophysical behavior and reservoir characteristics including the same porosity-permeability best-fit line and the same range of the DRT values. It is based on the master plot for the permeability against porosity supported with the DRT ranges. The Triassic reservoir samples were classified into six PSRTs, each with a reliable best-fit line ($R2 \geq 0.780$) and a defined range of DRT values. The PSRT1 group has the highest DRT range (16.1-22.1) and the highest contribution of the porosity to the reservoir permeability ($R2 \geq 0.832$); it is primarily composed of Sandstone facies. On the other side, the lowest porosity contribution to the permeability is the main character of the PSRT6 ($R2 \geq$ 0,740), which is characterized by the where; DRT is the discrete rock type (Shenawi et al., 2007; Shehata et al., 2021), is the effective helium porosity, k is the measured permeability, R35 is the effective pore radius (Winland, 1972); RQI is the reservoir qulaity index; FZI is the flow zone indicator; and RPI is the reservoir potentiality index (Nabawy and El Sharawy, 2018). PSRTs refer to the dominant petrophysicla static rock type

The PSRT2-3 samples are characterized by lower reservoir quality than the PSRT1 (Table ;) they are characterized by lower porosity and permeability (av. □ and av. k equal 6.97 % & 83.5 mD, and 8.93 % & 37.8 mD, respectively, Table 03.1). Their reservoir quality is still promising due to their rock compositions, which are dominated by the Grey sandstone medium, sometimes coarser and Grey sandstone medium, facies. The PSRT1-3 samples are primarily affected by the reservoir quality-supporting diagenetic features (dissolution and fracturing, with various intensities.

On the other side, the PSRT6 has the lowest porosity contribution to permeability and the lowest DRT range It is composed primarily of the Fine to very fine sandstone, sometimes medium light grey compact hard sandstone with clay and Grey clay becoming brown red Intercalation of dcm of grey sandstone facies. The PSRT5-6 samples are more similar to the PSRT6 samples than those of the other PSRTs, i.e., they are less promising than the PSRT2-3 samples which are composed of Grey sandstone medium, sometimes coarser facies. This low reservoir quality is due to their implementation by the pressure solution and Mechanical Compaction silica and Calcite cementation and authigenic mineral content The highly reliable best-fit lines of the porosity-permeability relationships of the Barkawi bin Kahla samples enable the estimation of k in terms of ∅ as follows.

PSRT1: $k = 1.38\ \varnothing^{2.67}$	$(16.1 \leq DRT \leq 22.1)$	$(R^2 = 0.832)$
PSRT2: $k = 0.139\ \varnothing^{3.08}$	$(15.1 \leq DRT \leq 16.0)$	$(R^2 = 0.983)$
PSRT3: $k = 0.029\ \varnothing^{3.114}$	$(13.1 \leq DRT \leq 15.0)$	$(R^2 = 0.648)$
PSRT4: $k = 0.007\ \varnothing^{3.115}$	$(12.1 \leq DRT \leq 13.0)$	$(R^2 = 0.956)$
PSRT5: $k = 0.002\ \varnothing^{3.116}$	$(11.1 \leq DRT \leq 12.0)$	$(R^2 = 0.948)$
PSRT6: $k = 0.0009\ \varnothing^{2.89}$	$(5.5 \leq DRT \leq 11.0)$	$(R^2=0.748)$

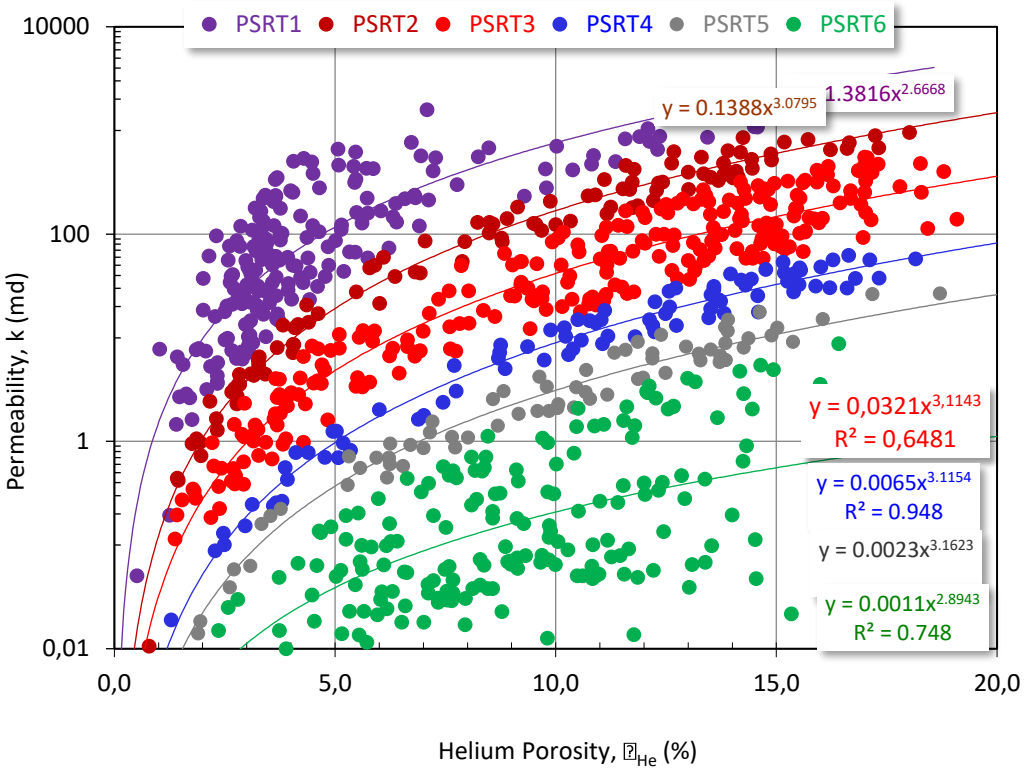

Fig 12: Rock typing the reservoirs seuqence in Barkawi bin Kahla Basin based on ∅-k-DRT data.(**Source: Excel, company documents**)

2.4. Implication of the Effective Pore Size (R35) on k and eff

Despite permeability is dependent on porosity, its dependence on the effective pore radius (R_{35}) of Winland (1972) is mentioned in some literature (Teama and Nabawy, 2016; Nabawy et al., 2018a, b; El Aal and Nabawy, 2019; Lai et al., 2020; Abuhagaza et al., 2021; Radwan and Nabawy, 2022). Permeability of the Barkawi bin Kahla samples is ranked as tight to excellent values (0.02-5496 mD, Fig. 03.6a, Table 03.1); it is primarily dependent on the R_{35} values, which are ranked as micro to mega pores/fractures, with highly reliable exponential relationships ($R_2 \geq 0.874$, Fig. 03.6a) for the various PSRTs. The PSRT1-2 samples have mega pores/fractures and macro pores, while the PSRT6 group has meso to macro pore throats. However, the petrographical description indicates a high degree of compaction, micro intergranular pores, and fractures/channels (Fig. 03.2a, b). This states that the estimated relatively high pore throat radius is primarily attributed to the presence of fractures and channels

as highly conductors' conduits Permeability could be estimated in terms of R_{35} as follows.

PSTR1: $R_{35} = 256.6\ k^{0.32}$ $(R^2 = 0.874)$

PSTR2: $R_{35} = 163.0\ k^{0.31}$ $(R^2 = 0.987)$

PSTR3: $R_{35} = 100.1\ k^{0.34}$ $(R^2 = 0.940)$

PSTR4: $R_{35} = 70.8\ k^{0.32}$ $(R^2 = 0.970)$

PSTR5: $R_{35} = 55.1\ k^{0.33}$ $(R^2 = 0.967)$

PSTR6: $R_{35} = 41.8\ k^{0.37}$ $(R^2 = 0.899)$

The exponential values of the R_{35}-k relationships fluctuate about 0.33 due to the similarity in mineral composition, while the difference in the multiplication factors is due to the difference in the pore architecture and size (Fig. 03.6a). Also, the R35 is exponentially related to the porosity values (pore volume) with poor to very highly reliable relationships ($0.436 \leq R^2 \leq 0.941$, Fig. 03.6b). The scattered PSRT1 and PSRT6 samples are due to variation of the pore aperature sizes. This plot declares the various contributions of the pore volume to the effective pore radius based on its PSRT number and reservoir quality. The R35 can be also estimated in terms of ∅ using the following mathematical model.

PSTR1: $R_{35} = 348.8\ \varnothing^{0.70}$ $(R^2 = 0.499)$

PSTR2: $R_{35} = 90.3\ \varnothing^{0.95}$ $(R^2 = 0.941)$

PSTR3: $R_{35} = 35.9\ \varnothing^{0.95}$ $(R^2 = 0.709)$

PSTR4: $R_{35} = 15.0\ \varnothing^{0.97}$ $(R^2 = 0.858)$

PSTR5: $R_{35} = 8.17\ \varnothing^{0.99}$ $(R^2 = 0.840)$

PSTR6: $R_{35} = 4.60\ \varnothing^{0.90}$ $(R^2 = 0.436)$

From this model, it is indicated that the exponential values almost approach the unity for the various PSRTs, while the multiplication factors are impressive indicators for the reservoir quality where they increase from the PSRT6 (4.60) to the PSRT1 (348.8). This may be attributed to increasing the pore connectivity as an implication for the predominating the reservoir quality-supporting diagenetic features while decreasing the R_{35} and the pore connectivity of the PSRT6 samples is due to the dominance of compaction, cementation, and increasing the authigenic minerals.

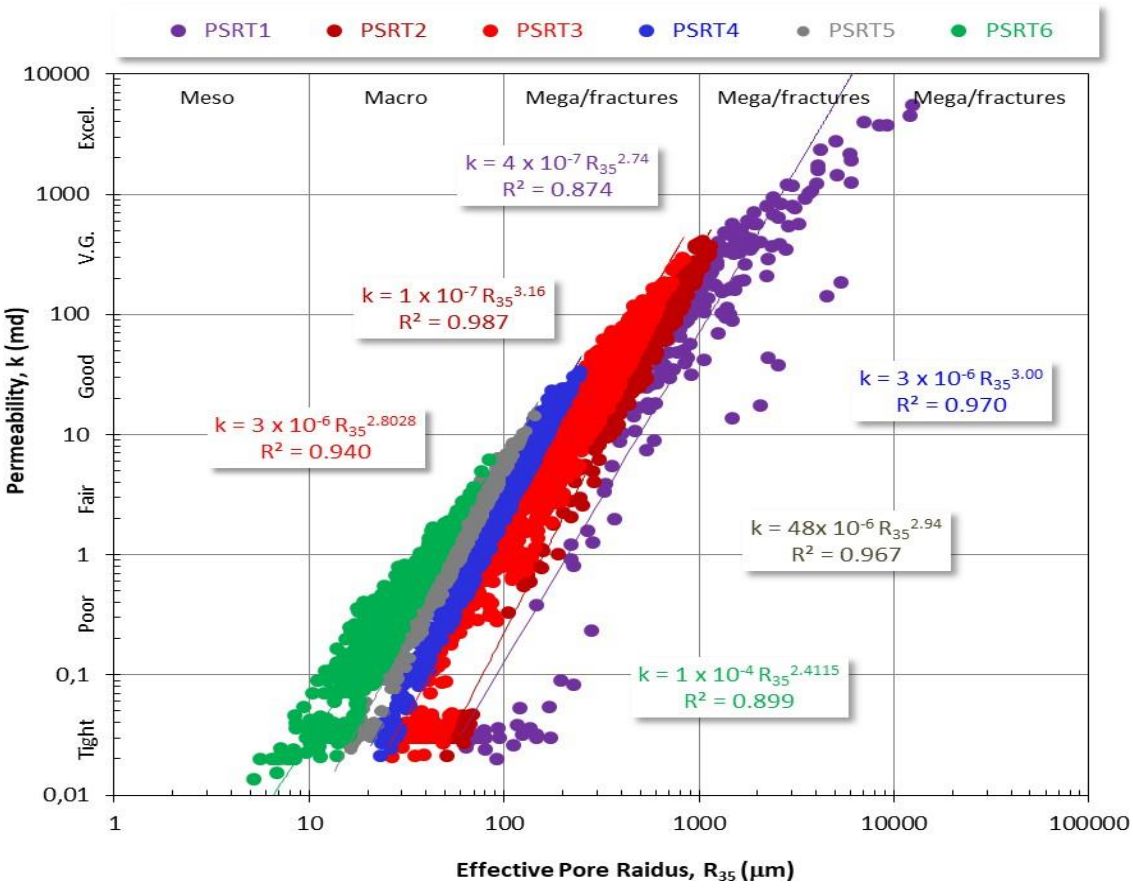

Fig. 13: Plotting the effective pore radius (R_{35}) versus a) the permeability (k), and b) the effective porosity (∅) of the studied reservoirs sequence.
(**Source: Excel, company documents**)

2.5. RQI attributes

The efficiency of the reservoir quality index (RQI) values of the Barkawi bin Kahla reservoirs and their rank are primarily attributed to their flow and storage capacities that are mostly contributed by the porosity, permeability, and the effective pore radius (R35) (Fig. 03.7 RQI). The RQI is controlled by the porosity values of the various PSRTs in a set of exponential relationships (0.9537 □ R2 □ 0.9967, Fig. 03.7a RQI).

Plotting the RQI as a function of k indicates that k is a main attribute for the RQI, which is exponentially related to the permeability (RQI). Some disturbance is noticed in the PSRT6 and characterized by poor porosity values, with different pore types including porosity.

Plotting the RQI values versus the R35 indicates that its main attribute in addition to the permeability, where the RQI is exponentially related to the R35 with very high reliability (0.9664 □ R2 □ 0.9975). This may be attributed to the fact that permeability is primarily controlled by the R35 and the RQI in turn is controlled by the permeability, i.e., the RQI is mainly controlled by the R35 (Fig. RQI).

Consequently, the RQI values are primarily controlled by the permeability and the effective pore radius (R35) in addition to its fair dependence on porosity due to the complexity of the pore throat architecture of some samples, especially of the PSRT1 and the PSRT6. Based on the high reliability of the obtained mathematical models, the RQI can be estimated in terms of its corresponding petrophysical values as follows.

PSTR1:	$RQI = 0.37 \varnothing^{0.83}$	$(R^2 = 0.659)$
	$RQI = 0.2687\ k^{0.3738}$	$(R^2 = 0.9248)$
	$RQI = 0.0021\ R_{35}^{0.9247}$	$(R^2 = 0.966)$
PSTR2:	$RQI = 0.1179 \varnothing^{1.0373}$	$(R^2 = 0.968)$
	$RQI = 0.2261 k^{0.3397}$	$(R^2 = 0.996)$
	$RQI = 0.0009\ R_{35}^{1.0863}$	$(R^2 = 0.997)$
PSTR3:	$RQI = 0.0563 \varnothing^{1.0573}$	$(R^2 = 0.858)$
	$RQI = 0.1741\ k^{0.3508}$	$(R^2 = 0.986)$
	$RQI = 0.0014\ R_{35}^{1.0409}$	$(R^2 = 0.990)$
PSTR4:	$RQI = 0.0239 \varnothing^{1.0962}$	$(R^2 = 0.954)$
	$RQI = 0.14\ k^{0.35}$	$(R^2 = 0.9956)$

$RQI = 0.0015\ R_{35}^{1.0652}$ ($R^2 = 0.9968$)

PSTR5: $RQI = 0.016\ \varnothing^{1.0427}$ ($R^2 = 0.941$)

$RQI = 0.1193\ k^{0.3424}$ ($R^2 = 0.994$)

$RQI = 0.0016\ R_{35}^{1.0741}$ ($R^2 = 0.9955$)

PSTR6: $RQI = 0.0087\ \varnothing^{0.7196}$ ($R^2 = 0.7196$)

$RQI = 0.0941\ k^{0.4343}$ ($R^2 = 0.9537$)

$RQI = 0.00393R^{0.8789}$ ($R^2 = 0.986$)

Correlating the reliability of this equations set indicates that the reliability (R2) of the RQI relationships increases from the RQI-□ to the RQI-R35 which ensures that □, k, and R35 contribute to the RQI in an ascending order based on its contribution intensity.

Similar to the R35-□ plot (Fig.), the exponential values fluctuate around the unity, i.e., the multiplication values are a good indicator for the reservoir quality, which increases from 0.0087 for the PSRT6 to 0.1179of the PSRT2 samples (Fig. RQI

Correlating the reliability of this equations set indicates that the reliability (R2) of the RQI relationships increases from the RQI-∅ to the RQI-R35 which ensures that ∅, k, and R35 contribute to the RQI in an ascending order based on its contribution intensity.

Similar to the R_{35}-∅ plot (Fig. 03.6b), the exponential values fluctuate around the unity, i.e., the multiplication values are a good indicator for the reservoir quality, which increases from 0.009 for the PSRT6 to 0.37 of the PSRT1 samples (Fig. 03.7a).

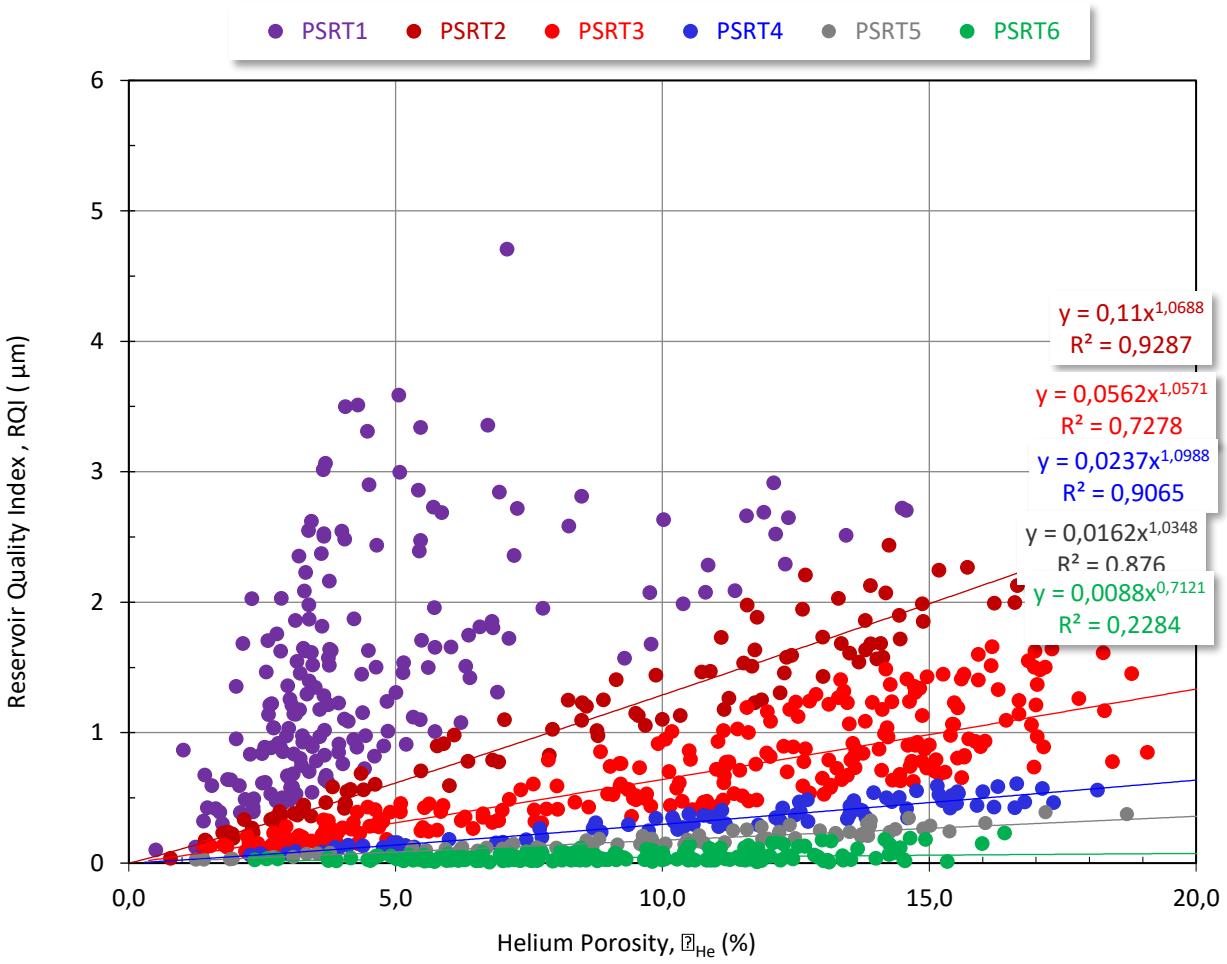

Fig. 14: Analysis of the ΦHe–RQI Relationship Across Six Sandstone Types Using Power-Law Fitting Curves

Source: Excel, company documents

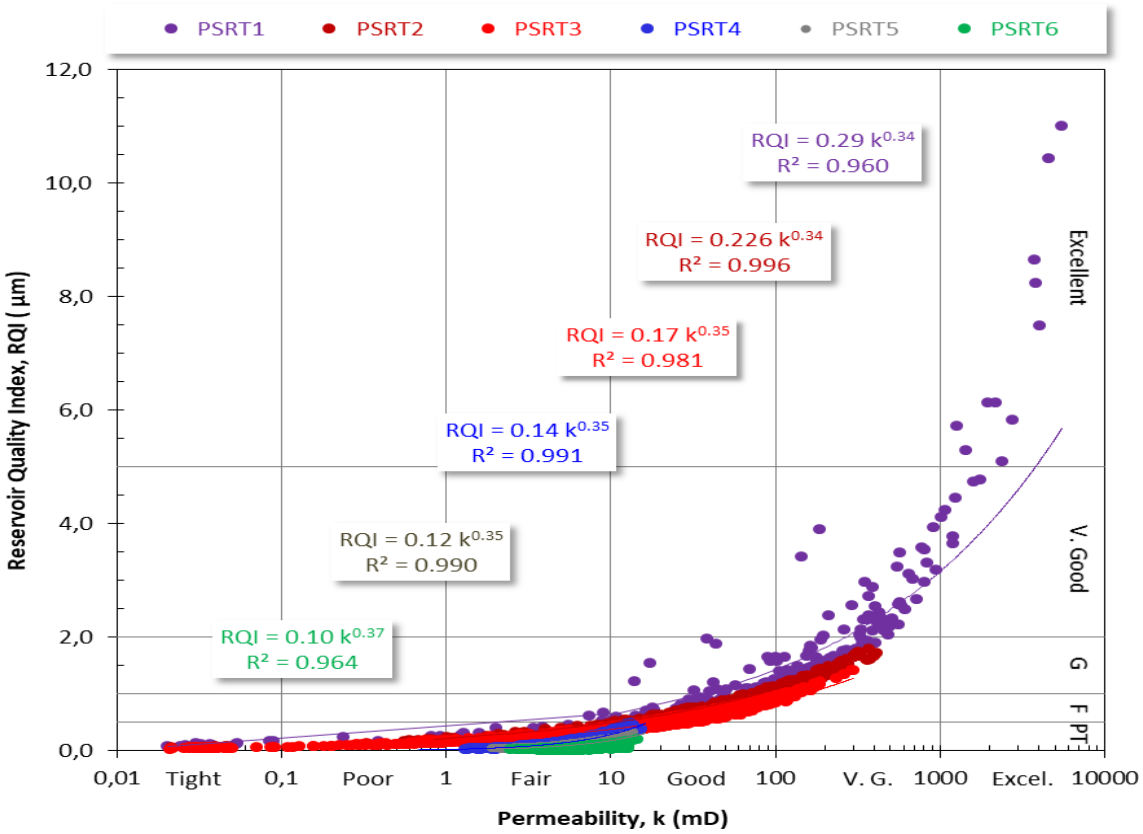

Fig. 15: Relationship Between Permeability (k) and Reservoir Quality Index (RQI) for Different Sandstone Types (PSRT1–PSRT6)
Source: Excel, company documents

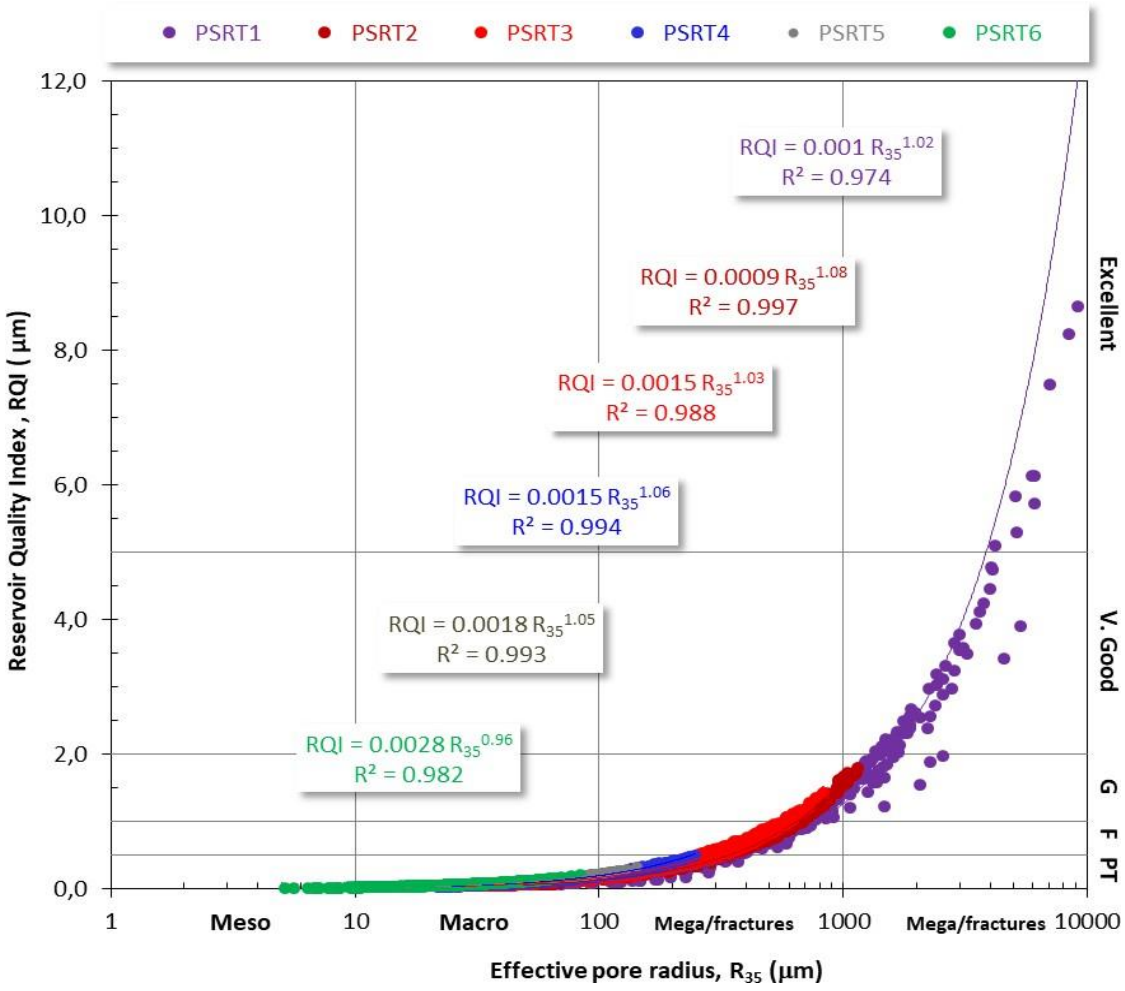

Fig. 16: Plotting the reservoir quality index of the studied PSRTs versus their contributors

a) porosity (∅), b) permeability (k), and c) Effective pore radius (R_{35}). G, F, P, and T mean good, fair, poor and tight reservoir quality ranks. Classification ranks are following Nabawyand El Saharawy (2018). (**Source: Excel, company documents)**

2.6. FZI attributes

The FZI is among the reservoir quality parameters but it is a more complicated parameter than the RQI. This complexity is due to its dependence on the pore-to-grain ratio (NPI). It has been mentioned by many authors (e.g., Nabawy et al., 2020b; 2023; Radwan et al., 2023).

In addition,

for the Benkahla, the sandstone reservoirs are highly complicated, in particular the PSRT1 and PSRT6 which are characterized by matrix porosity and fractures, respectively. Plotting the FZI values versus the porosity indicates that the FZI values of the PSRT1 samples have mega pores and fractures, while the PSRT6 is characterized by poor and tight pore throats. This plot indicates that the FZI is highly scattered and can't be modeled in terms of porosity due

to its scattering (Fig. 03.8a). Plotting the FZI against the permeability is a useful plot fordiscriminating the studied PSRTs into two groups; fair to excellent for the PSRT1-3 samples which are characterized by macro to mega pores, and fair to tight for the PSRT4-6 which are characterized by the lowest reservoir quality (Fig. 03.8b). This discrimination is accompanied with fair permeability due to the presence of some vertical microfractures. Plotting the FZI as a function of the R35 (Fig. 03.8c) indicates a somewhat fair direct proportional relationship between the FZI and the R35; however, this dependence has low reliability (R2 □ 0.36) and cannot be modeled. Theoretically, the FZI should be dependent on the porosity, permeability, and the effective pore radius, but practically these relationships are more or less scattered due to the heterogeneity in the pore throat architecture as revealed from the petrographical study . However, summing up the various PSRTs compensated for this scattering and enabled modeling of this relationship but for the whole samples, not for a definite PSRT.

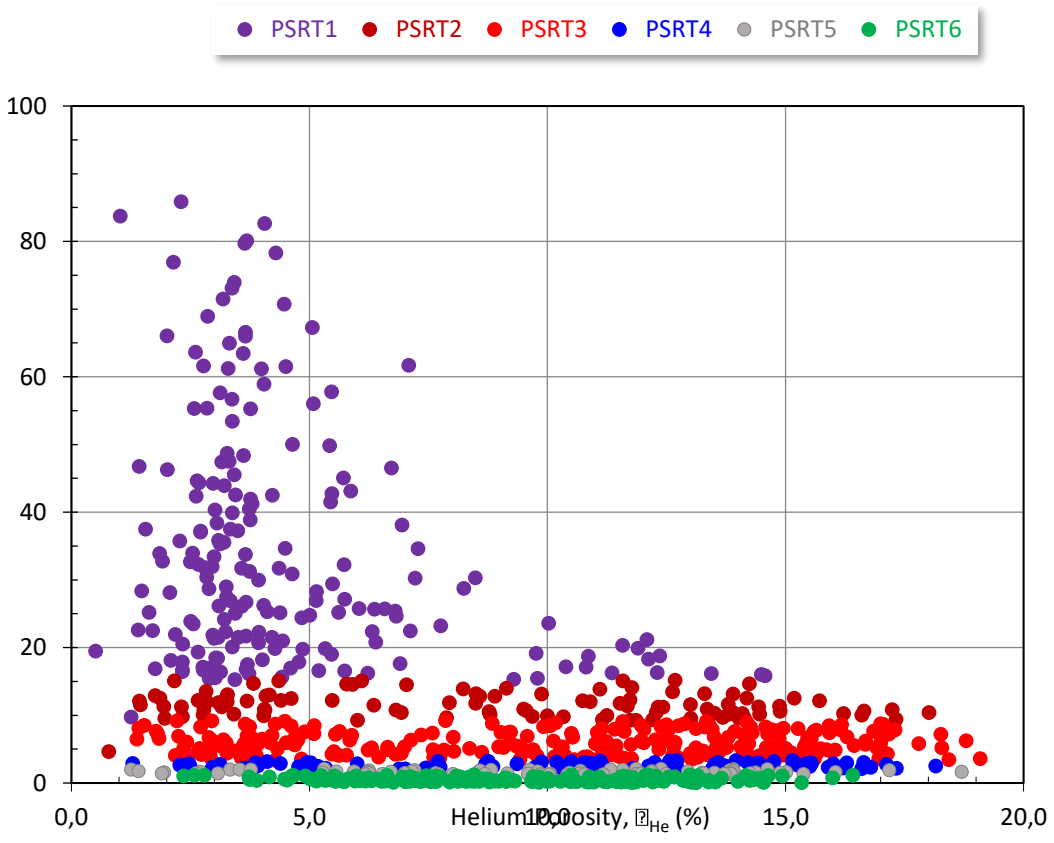

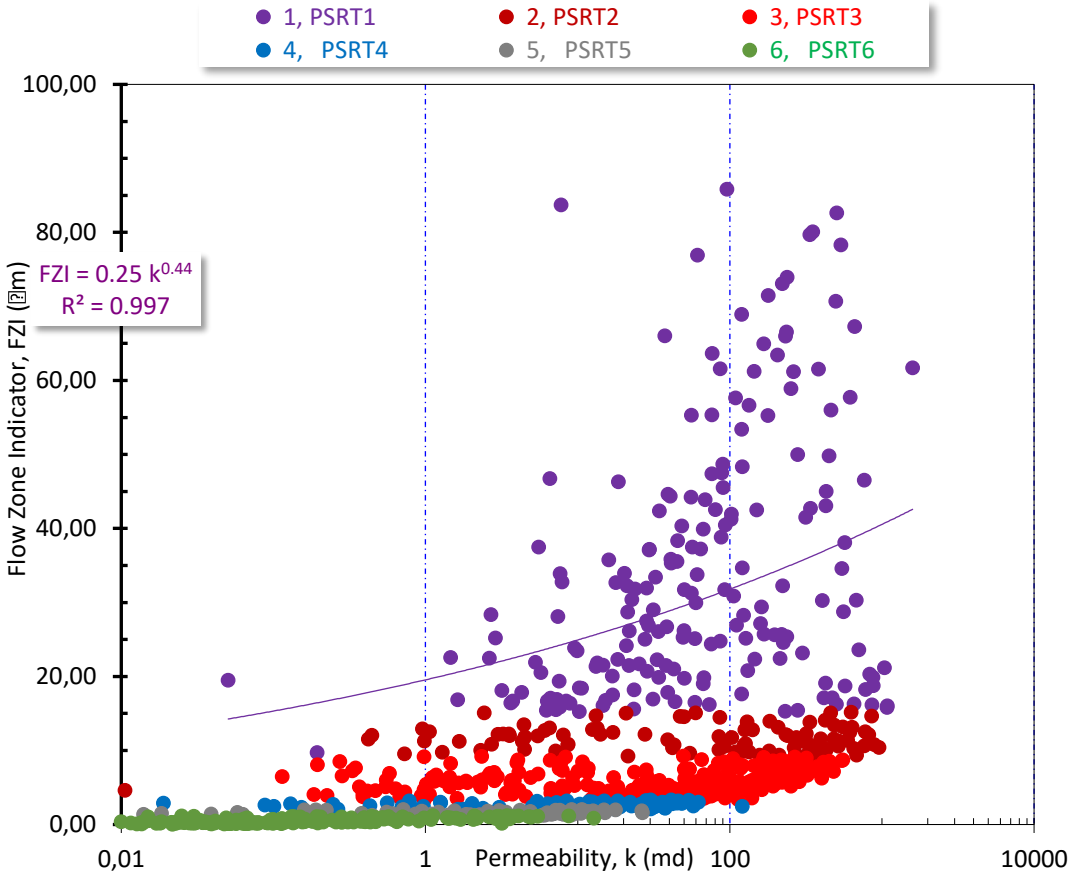
1, PSRT1
2, PSRT2
3, PSRT3
4, PSRT4
5, PSRT5
6, PSRT6
100,00
80,00
60,00
40,00
20,00
0,00
FZI = 0.25 k^0.44
R² = 0.997
Flow Zone Indicator, FZI (m)
0,01
1
Permeability, k (md)
100
10000

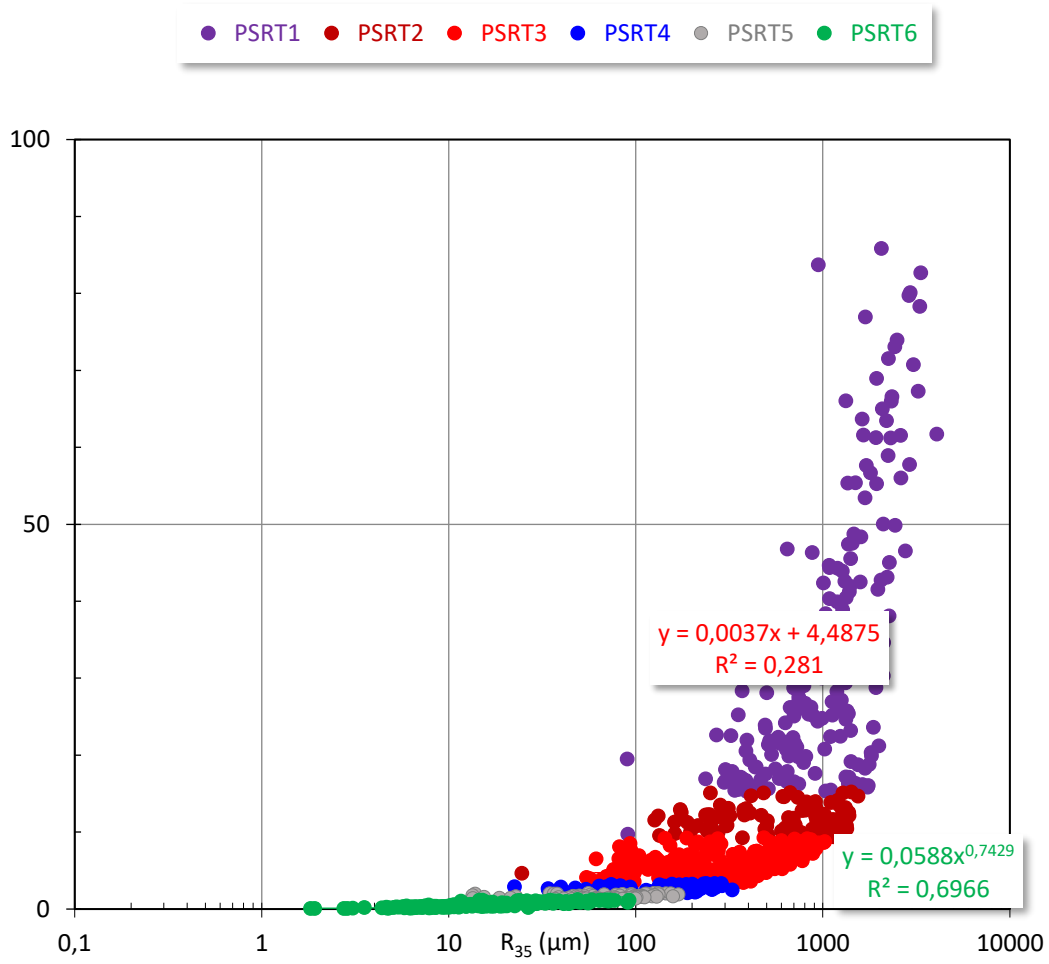

Fig. 17: Plotting the flow zone indicator of the studied PSRTs versus their contributors a) porosity (□), b) permeability (k), and c) Effective pore radius (R35). **(Source: Excel, company documents)**

2.7. Reservoir ranks of the various PSRTs

To verify the efficiency of the rock classification process, the Rock Quality Index (RQI) and the Rock Quality Index (NPI) are compared with each other, supported by FZI break lines as shown in Figure 3.9a, demonstrating high rock classification efficiency for the Ben Kahla reservoirs. This indicates that the PSRT reservoirs are separated by FZI break lines = 16.05, 9.25, 3.39, 2.065, and 1.25 µm. It is noted that both PSRT5-6 reservoirs have poor to tight reservoir quality, while PSRT4 has medium quality, PSRT3 has good quality, and PSRT1-2 has very good to excellent reservoir quality (Figure 3.9a). This reservoir quality classification chart is supported by the RQI-FZI chart, which indicates that PSRT1 reservoir quality is tight to excellent, i.e., its quality and pore structure are highly variable (Figure 3.9b). The same applies to PSRT2-3 reservoirs, which have a tight to good quality, while PSRT4-6 reservoirs have a poor to tight quality, ensuring the highly heterogeneous nature of the pore structure of the Ben Kahla Barkawi reservoirs.

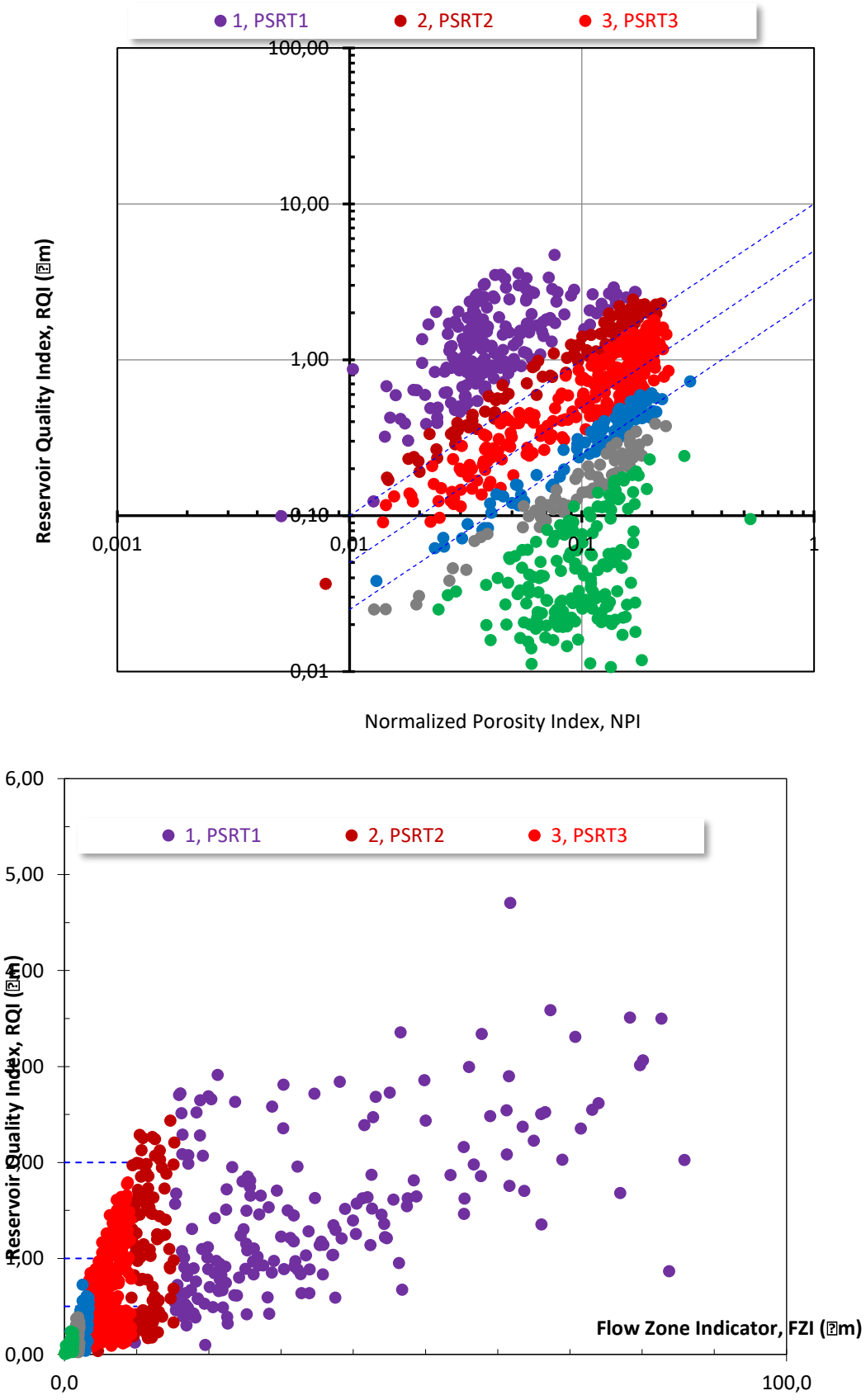

Fig 18: Plotting the reservoir quality index (RQI) of the PSRTs versus a) the

NPI, and b) the FZI values. mean good, fair, poor and tight reservoir quality ranks **(**Classification ranks are following Nabawy and El Saharawy (2018). (**Source: Excel, company documents)**

2.8. Reservoir zonation into HFUs

Dividing the reservoir into several HFUs based on core data is a key protocol, essential for compiling the outputs of this research at the well scale, where core data versus depth are presented in log format (Figure 3.10a-c). The interval extracted from the Triassic Ben Kahla core is divided into six main units in different wells with □ = 5% and k = 1.0 mD as threshold values. These units in well W02 cannot be divided into further HFUs due to their heterogeneity and spiky behavior, as shown in their PSRT configuration (PSRT3-6, last track, Figure 3.10a). The SI is characterized by very good reservoir quality. The presence of a very high and abnormal FZI (track 4, Figure 3.10a) is attributed to the dominance of vertical microfractures, as reported by Nabawi and Sahrawi (2018). The very high R35 values (Trajectory 5, Figure 3.10b) are also attributed to the dominance of microfractures and shale lineations. However, the storage capacity of Triassic-age reservoirs in this well ranges from negligible to acceptable.

Similar to the well, the reservoir sequence in the well consists primarily of PSRT3 (Figure 3.10c). The basal portions of the sequence (SI) have higher porosity, permeability, RQI, FZI, and R35 values than the upper portions. However, the entire sequence is promising with porosity and permeability significantly higher than the cutoff values (Trajectories 1-2, Figure 3.10c). However, the Rock Quality Index (RQI) and Rock Quality Index (FZI) values indicate poor to good reservoir quality (Trajectories 3-4). The entire sequence is characterized by large and wide pores, thanks to the dominance of microfractures and shale lineations, responsible for the thorny behavior of petrophysical and reservoir parameters.

(a) OKS30 Well

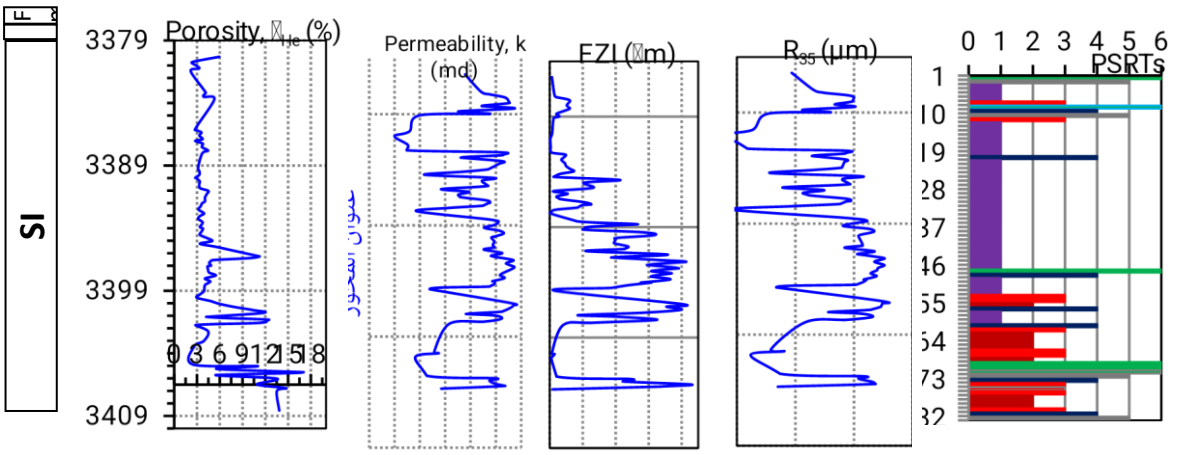

(b) OKS32 Well

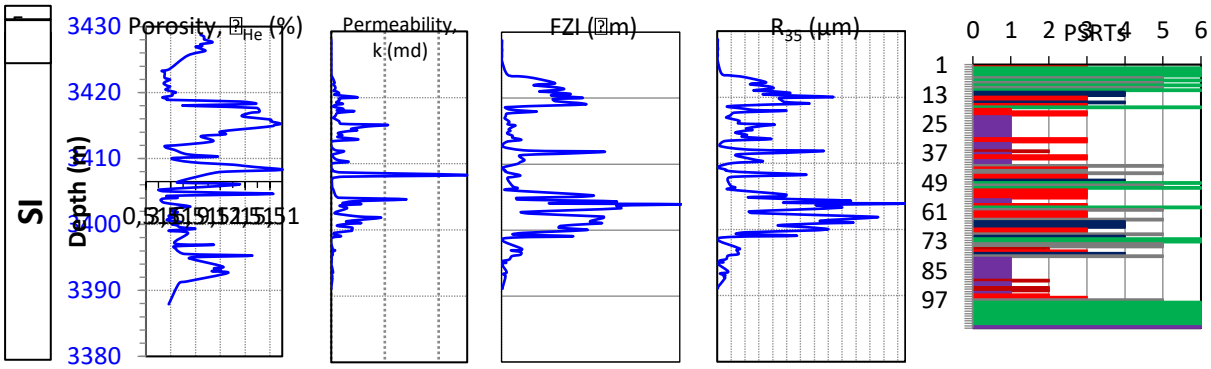

(c) OKS35 Well

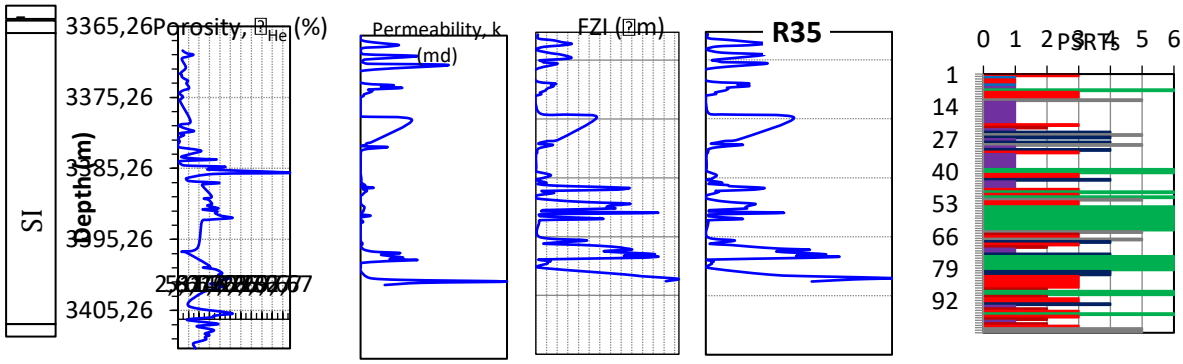

(d) OKS39 Well

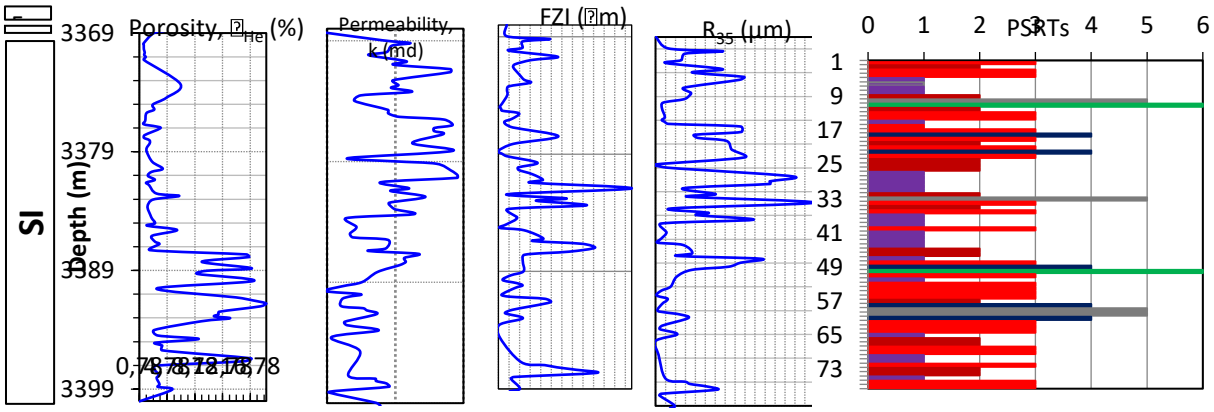
SI
Depth (m)
3369
3379
3389
3399
Porosity, ϕ_{He} (%)
Permeability, k (md)
FZI (µm)
R_{35} (µm)
0 1 2 3 4 5 6
PSRTs
1
9
17
25
33
41
49
57
65
73

(f) OKS40 Well

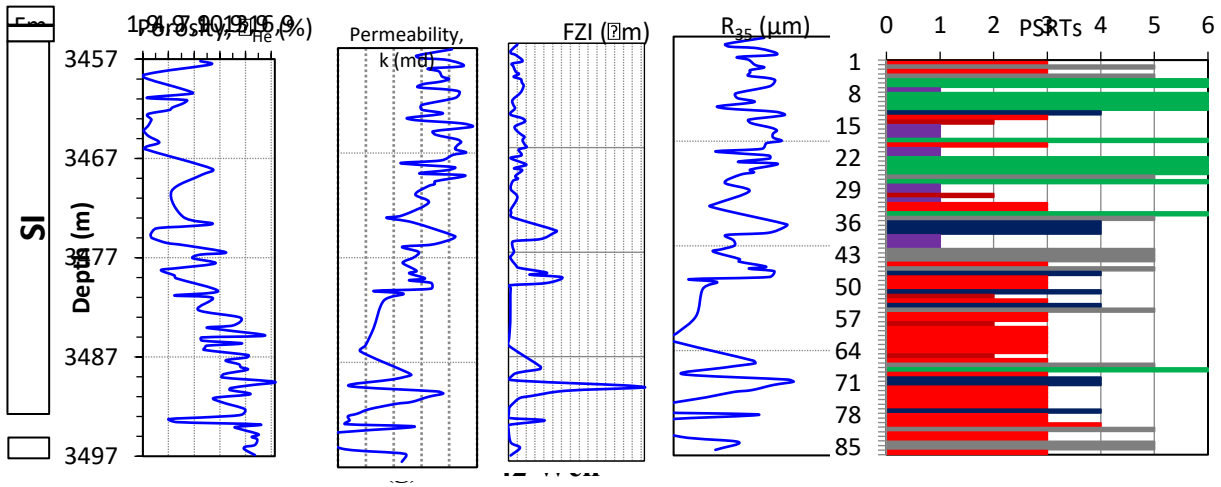

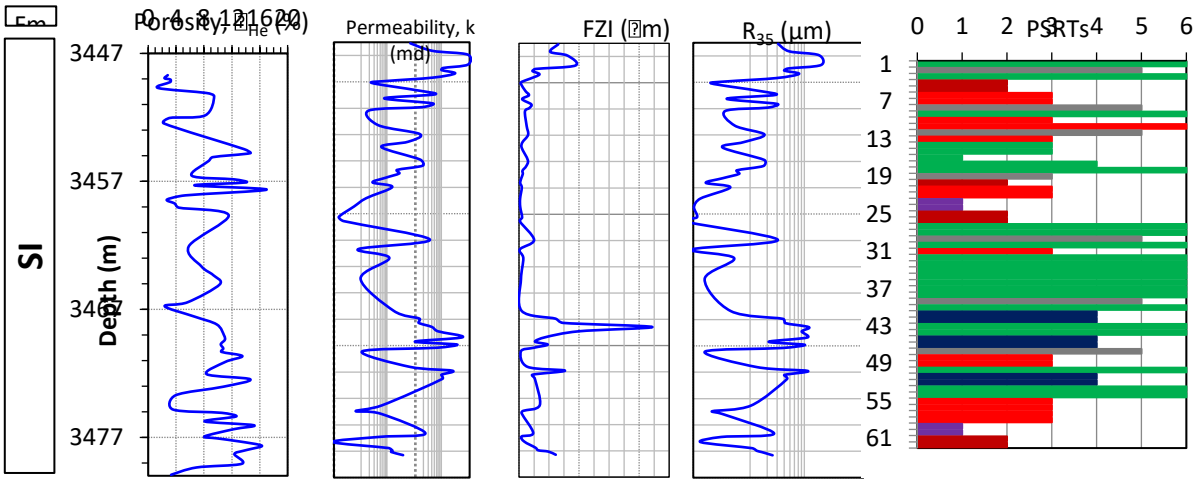

(h) OKS43 Well

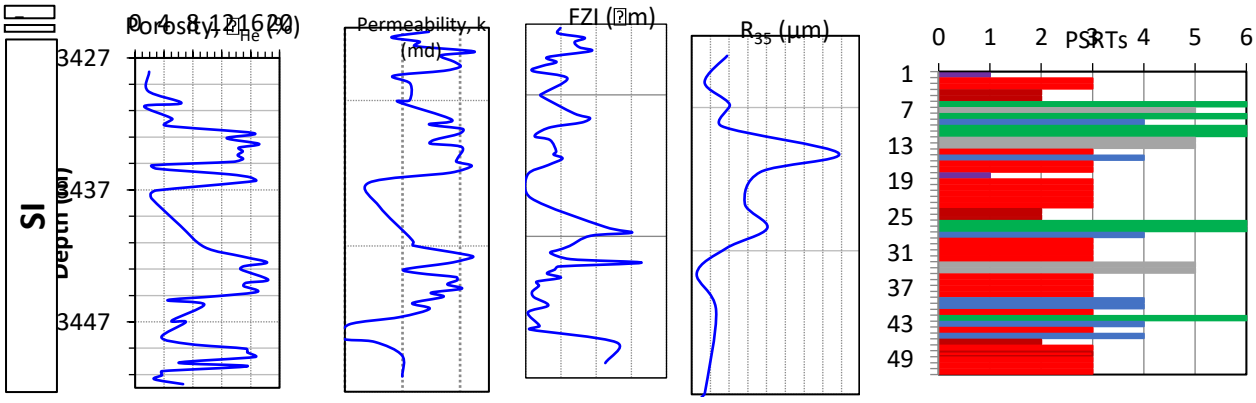

(i) OKS44 Well

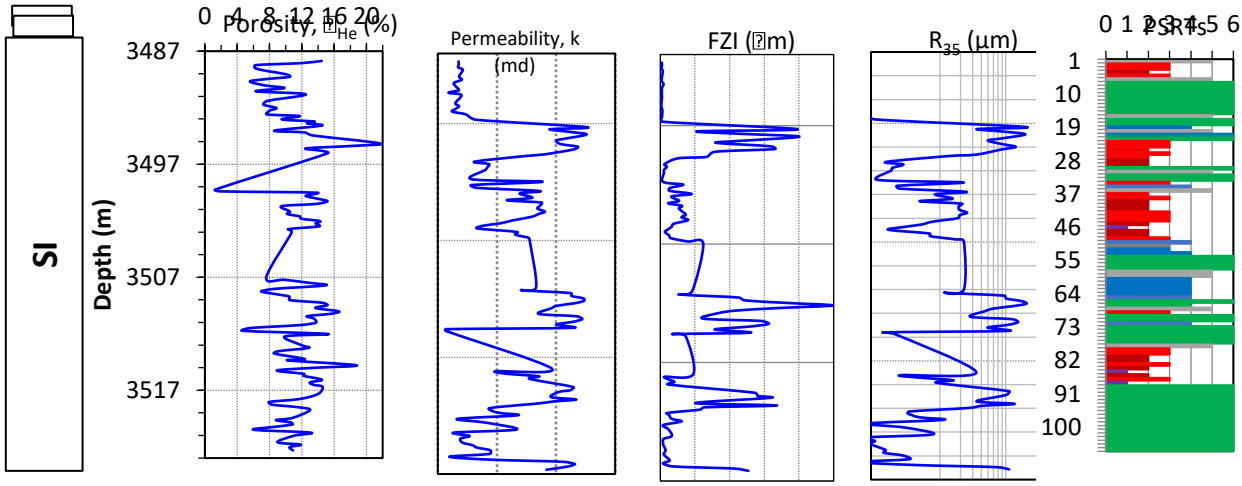
SI
Depth (m)
3487
3497
3507
3517
0 4 8 12 16 20
Porosity, He (%)
Permeability, k (md)
FZI (m)
R35 (µm)
0 1 2 3 4 5 6
PSRTs
1
10
19
28
37
46
55
64
73
82
91
100

(k) OKS45 Well

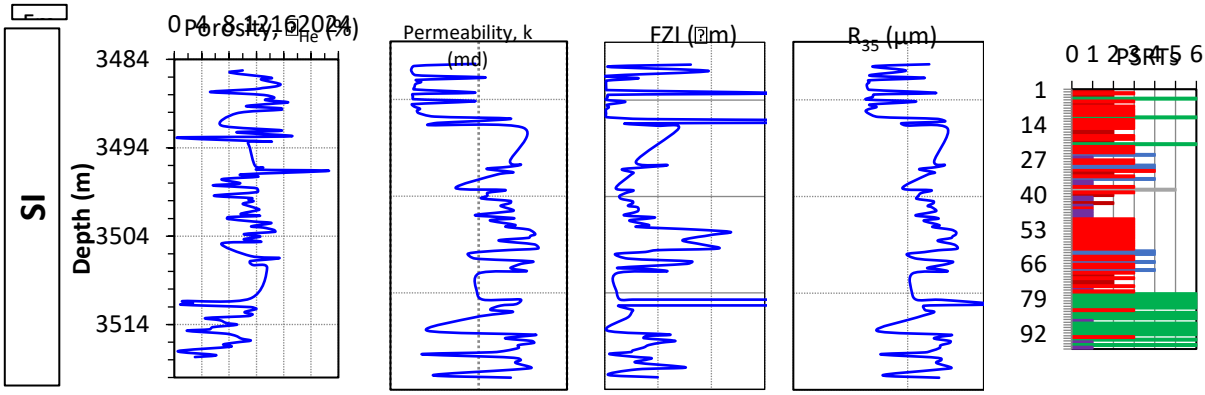
SI
Depth (m)
3484
3494
3504
3514
0 4 8 12 16 20 24
Porosity, He (%)
Permeability, k (md)
FZI (m)
R35 (µm)
0 1 2 3 4 5 6
PSRTs
1
14
27
40
53
66
79
92

Conclusion General

Conclusion General

The Ben Kahla field, located in the Oued Mya depression in the central Triassic region of Algeria, represents the most explored area in this basin. This area lies between the Hassi R'Mel fields to the northwest and the Hassi Messaoud fields to the east.

The field's primary petroleum importance is related to the presence of Triassic reservoirs. The Paleozoic and Triassic targets are located at great depths, ranging from 3,400 to 4,000 meters. Within the Triassic, the primary target is the Lower Series.

The primary source rocks of the Triassic reservoirs in the Ben Kahla field are radioactive Silurian clays. The regional coverage of the Triassic reservoirs consists of Triassic (Salt S4) and Liassic (Levels S3 to S1) evaporite deposits.

The primary target is the Lower Series. Both the log and petrophysical interpretation, as well as the summary description of the core sample, confirm that the lower reservoir sequence remains entirely within the oil-bearing part, above the oil-water contact point, with an average reservoir pressure of 442 kg/cm³.

The petrophysical analysis of the Triassic reservoir sequence in the Benkahla Basin reveals the presence of six PSRTs, each characterized by distinct petrophysical and facies types.

- PSRT1-3 show promise as reservoirs due to lower levels of authigenic clay content, while PSRT4-5 exhibit poorer characteristics, and PSRT6 is deemed unpromising.

- Several mathematical models have been introduced to estimate parameters such as R35 (expressed in terms of ϕ and k, with $0.436 \leq R2 \leq 0.987$), RQI (in terms of ϕ, k, and R35, with $0.569 \leq R2 \leq 0.997$), and FZI (in terms of the effective pore radius R35, with $R2 = 0.796$).

Bibliographie

1. Amaefule, J.O. et al. (1993) – Enhanced Reservoir Description Using Core and Log Data.
2. Ben Baba, A., Nagazi, A., 2013. Characterization and modeling of the northeastern part of the Barkaoui Basin field (Professional project for the end of the IAP training).
3. Bigol, MA, 2013. "Late logging: Petrophysical and geological interpretation." IAP course.
4. Boudjemaa, R., 1987. Structural evolution of the Triassic oil basin in the northeastern Sahara. PhD thesis, University of Paris-Sud, Orsay.
5. Kahol, F., 2004. Rock logging and spectroscopy (NGS) of Triassic tectonic sequence characteristics (Oued Mia basin, central Sahara). Master's Thesis, 84 pages, International Petroleum Research Institute, Algeria.
6. Maysa Murad. 2009. Petrophysical Characterization Study and Re-evaluation of the Reserves of the Triassic Sandy-Sandy Reservoir (Lower Series) of the Ben Kahla Deposit. Oued Mya Basin, Engineering Thesis.
7. Petroleum Research Institute/Sonatrach. 1997. Regional structure of Triassic reservoirs in Algeria. Vol. Journal of Geology B. Reference: PEP 43 719-1B.
8. Schlumberger. 2013. "Practical Guide to Petrol Gas."
9. Schlumberger (1989) – Log Interpretation Principles.
10. Serra, A. 1979. Delayed Logging, Logging Data Collection, Volume 1, SNEAP. P PAU-France.
11. Serra, O. 1979. Delayed Logging, Basis for Interpretation of Logging Data, Volume 2, SNEAP. P PAU-France.
12. Sonatrach. Mud Logging Final Report - Well.
13. Sonatrach. Petrophysical Analysis Reports of Benkhla Wells.
14. Sonatrach. Well Core Description Reports for the Benkhla Field.
15. Sonatrach. Well Completion Reports.
16. Thouvenin, J., 1968. Laboratory study of sediments - Permo-Triassic reservoir (Part II).
17. Tiab, D. & Donaldson, E.C. (2012) – Petrophysics.
18. WEC (Sonatrach-Schlumberger). 2007. "Well Evaluation Conference in Algeria.
19. Abdeen, M.M., Ramadan, F.S., Nabawy, B.S., El Saadawy, O., 2021. Subsurface structural setting and hydrocarbon potentiality of the Komombo

and Nuqra basins, south Egypt: a seismic and petrophysical integrated study. Nat. Resour. Res. 30 (5), 3575-3603.

20. Abuamarah, B.A., Nabawy, B.S., 2021. A proposed classification for the reservoir quality assessment of hydrocarbon-bearing sandstone and carbonate reservoirs: a correlative study based on different assessment petrophysical procedures. J. Nat. Gas Sci. Eng. 88, 103807.
21. Abuhagaza, A.A., El Sawy, M.Z., Nabawy, B.S., 2021. Integrated petrophysical and petrographical studies for characterization of reservoirs: a case study of Muglad Basin, North Sudan. Environmental Earth Sciences 80(5), 171
22. Aïfa, T., Zerrouki, A.A., Baddari, K., Géraud, Y., 2014. Magnetic susceptibility and its relation with fractures and petrophysical parameters in the tight sand oil reservoir of Hamra quartzites, southwest of the Hassi Messaoud oil field, Algeria Journal of Petroleum Science and Engineering 123, 120-137.

ملخص الدراسة

تهدف الدراسة إلى تقييم الخصائص الجيولوجية والبتروفيزيائية لحقل بنكحلة في حوض وادي ميا، الجزائر، لفهم إمكانيات المخزن الترياسي السفلي وتحديد جودة المخزن ووحدات التدفق الهيدروليكي (HFUs) لدعم الاستكشاف والإنتاج البترولي.

كشف تحليل عينات نوى من 10 آبار (OKS30 إلى OKS45) عن ستة أنواع صخرية بتروفيزيائية (PSRT1 إلى PSRT6)، مع تميز PSRT1 (حجر رملي بيج-أبيض) بأعلى جودة (مسامية 7.41%، نفاذية 795.375 ميلي دارسي). تم تقسيم المخزن إلى ست وحدات تدفق هيدروليكي، مع تأثير الكسور والطين على التغاير. تشير الدراسة إلى إمكانيات هيدروكربونية غير مستغلة (3–4 أضعاف الحجم المكتشف) في فخاخ هيكلية واستراتيغرافية.

الكلمات المفتاحية: حقل بنكحلة، حوض وادي ميا، مخزن ترياسي، تحليل نوى، أنواع صخرية بتروفيزيائية، مسامية، نفاذية، وحدات تدفق هيدروليكى، هيدروكربونات، فخاخ هيكلية

Résumé

L'étude vise à évaluer les caractéristiques géologiques et pétrophysiques du champ de Benkahla dans le bassin d'Oued M'ya, Algérie, afin de comprendre le potentiel du réservoir triasique inférieur, d'identifier la qualité du réservoir et de définir les unités d'écoulement hydraulique (HFUs) pour soutenir l'exploration et la production pétrolière.

L'analyse des carottes de 10 puits (OKS30 à OKS45) a révélé six types de roches pétrophysiques statiques (PSRT1 à PSRT6), le PSRT1 (grès beige-blanc) présentant la meilleure qualité (porosité moyenne de 7,41 %, perméabilité de 795,375 mD). Le réservoir a été divisé en six unités d'écoulement hydraulique, avec des fractures et des argiles influençant l'hétérogénéité. L'étude indique un potentiel d'hydrocarbures non exploité (3 à 4 fois le volume découvert) dans des pièges structuraux et stratigraphiques.

Mots-clés : Champ de Benkahla, Bassin d'Oued M'ya, Réservoir triasique, Analyse de carottes, Types de roches pétrophysiques, Porosité, Perméabilité, Unités d'écoulement hydraulique, Hydrocarbures, Pièges structuraux

Summary :
The study aims to assess the geological and petrophysical properties of the Benkahla field in the Oued M'ya Basin, Algeria, focusing on the Lower Triassic reservoir to determine its quality and define hydraulic flow units (HFUs) to support petroleum exploration. Core analysis from ten wells (OKS30 to OKS45) identified six petrophysical static rock types (PSRT1 to PSRT6), with PSRT1 (beige-white sandstone) showing a porosity of 7.41% and permeability of 795.375 mD. The reservoir was zoned into six flow units, with fractures and shales causing heterogeneity, indicating untapped hydrocarbon potential in structural and stratigraphic traps.

Keywords : Benkahla field, Oued M'ya Basin, Triassic reservoir, Core analysis, Petrophysical rock types, Porosity, Permeability, Hydraulic flow units, Hydrocarbons, Structural traps